



Contents lists available at ScienceDirect

European Journal of Medicinal Chemistry

journal homepage: <http://www.elsevier.com/locate/ejmech>

## Development of novel benzimidazole-derived neddylation inhibitors for suppressing tumor growth *in vitro* and *in vivo*

Xin Chen <sup>a,1</sup>, Xi Yang <sup>b,1</sup>, Fei Mao <sup>a,1</sup>, Jinlian Wei <sup>a,1</sup>, Yixiang Xu <sup>a</sup>, Baoli Li <sup>a</sup>, Jin Zhu <sup>a</sup>, Shuaishuai Ni <sup>b,\*\*</sup>, Lijun Jia <sup>b,\*\*\*</sup>, Jian Li <sup>a,c,d,\*</sup>

<sup>a</sup> State Key Laboratory of Bioreactor Engineering, Shanghai Key Laboratory of New Drug Design, East China University of Science and Technology, 130 Mei Long Road, Shanghai, 200237, China

<sup>b</sup> Cancer Institute, Longhua Hospital, Shanghai University of Traditional Chinese Medicine, Shanghai, 200032, China

<sup>c</sup> College of Pharmacy and Chemistry, Dali University, 5 Xue Ren Road, Dali, Yunnan, 671000, China

<sup>d</sup> Frontiers Science Center for Materiobiology and Dynamic Chemistry, East China University of Science and Technology, 130 Mei Long Road, Shanghai, 200237, China

### ARTICLE INFO

#### Article history:

Received 26 June 2020

Received in revised form

21 September 2020

Accepted 19 October 2020

Available online xxx

#### Keywords:

Neddylation

cullin1-Nedd8

Benzimidazole-derived inhibitor

Anticancer

### ABSTRACT

Ubiquitin-like protein neddylation is overactivated in various human cancers and correlates with disease progression, and targeting this pathway represents a valuable therapeutic strategy. Our previous work disclosed an antihypertensive agent, candesartan cilexetic (CDC), serves as a novel neddylation inhibitor for suppressing tumor growth by targeting Nedd8-activating enzyme (NAE). In this study, 42 benzimidazole derivatives were designed and synthesized based on lead compound CDC to improve the neddylation inhibition and anticancer efficacy. Optimal benzimidazole-derived **35** displayed superior neddylation inhibition in enzyme assay compared to CDC (IC<sub>50</sub> = 5.51 μM vs 16.43 μM), along with promising target inhibitory activity and killing selectivity in cancer cell. The results of cellular mechanism research combined with tumor growth suppression in human lung cancer cell A549 *in vivo*, accompanied with docking model, revealed that **35** has the potential to be developed as a promising neddylation inhibitor for anticancer therapy.

© 2020 Elsevier Masson SAS. All rights reserved.

### 1. Introduction

Cancer has become one of the most serious health issues for global public health [1]. According to a report from the World Health Organization (WHO) in 2018, cancer is the first or second leading cause of death before seventy years of age in 91 of 172 countries [2]. The GLOBOCAN 2018 database provides estimates of 18.1 million new cancer cases and 9.6 million cancer deaths worldwide [3]. Although the improvement of diagnostic methods has made significant progress in decreasing the tumor incidence and mortality, chemotherapy acts as one of the main anticancer

methods that still faces plenty of challenges, such as therapeutic resistance, monotonous research approaches, system toxicities and side effects. To overcome the defects and decelerate the spread of drug resistance, it is urgent to develop the next class of chemotherapeutics with novel mechanisms of action.

The ubiquitin proteasome system (UPS) acts as one of the most important protein degradation pathways that regulates the degradation of intracellular proteins, and it has important roles in a variety of cellular and organismal processes [4]. In the UPS, cullin-RING ubiquitin E3 ligases (CRLs) are the largest family of multiunit E3 ubiquitin ligases [5,6], which are assembled with the best-known cullin family members and activated by cullin neddylation [7,8]. Neddylation is a posttranslational modification of conjugating the neuronal precursor cell-expressed developmentally down-regulated protein 8 (Nedd8) to cullin family members and other noncullin substrates.

During the process of neddylation (Fig. 1A), Nedd8 first binds to Nedd8-activating enzyme (NAE) in an Mg<sup>2+</sup>/ATP-dependent manner [9,10] and then reacts to yield an acyl adenylate between the carboxyl terminus of Nedd8 and AMP (Nedd8-AMP) coupled

\* Corresponding author. State Key Laboratory of Bioreactor Engineering, Shanghai Key Laboratory of New Drug Design, East China University of Science and Technology, 130 Mei Long Road, Shanghai, 200237, China.

\*\* Corresponding author.

\*\*\* Corresponding author.

E-mail addresses: [nss1106@126.com](mailto:nss1106@126.com) (S. Ni), [ljjia@shutcm.edu.cn](mailto:ljjia@shutcm.edu.cn) (L. Jia), [jianli@ecust.edu.cn](mailto:jianli@ecust.edu.cn) (J. Li).

<sup>1</sup> These authors contributed equally to this work.

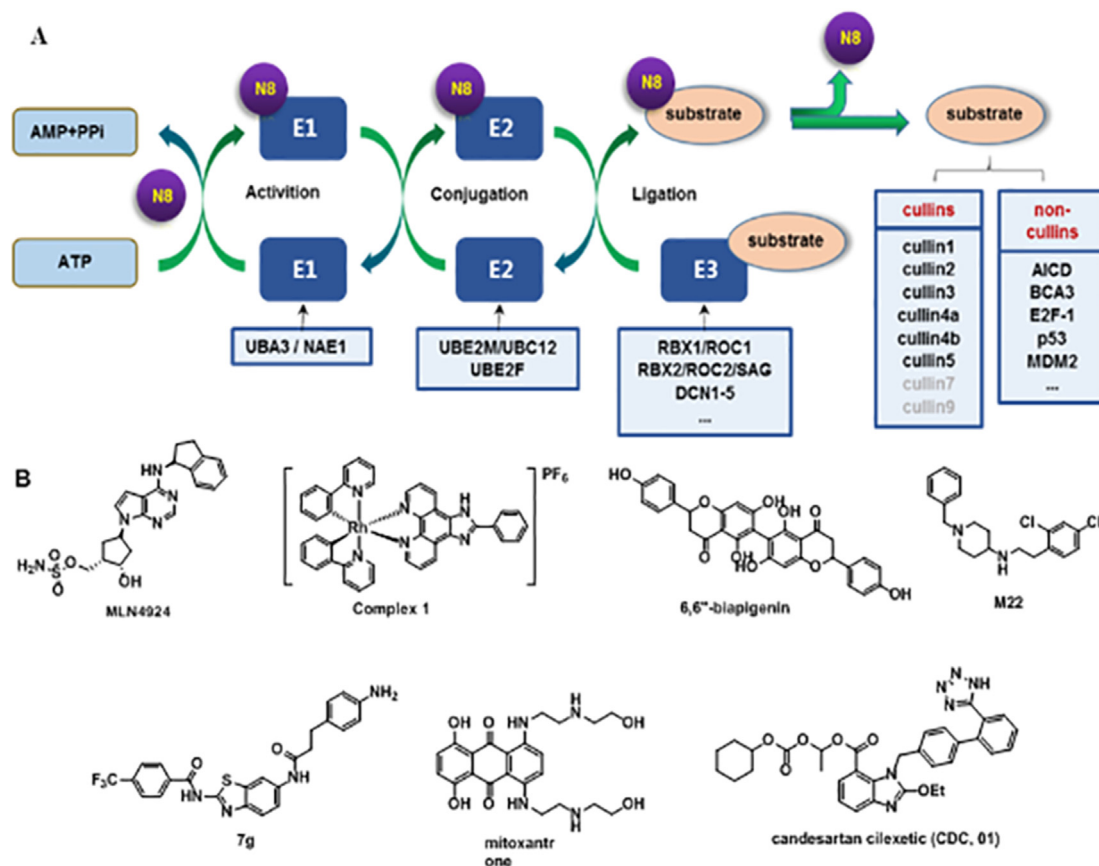


Fig. 1. The process of neddylation (A) and reported NAE inhibitors (B).

with the release of inorganic pyrophosphate. Nedd8-AMP reacts with the thiol of the active site cysteine residue in the NAE subunit to form a NAE-Nedd8 thioester and release AMP. Subsequently, Nedd8 is transferred to one of the two Nedd8 conjugating enzymes (UBE2M/Ubc12 [11] or UBE2F [12], E2s) through a transthioester reaction and forms E2-Nedd8. In the presence of Nedd8 ligases (E3s), Nedd8 is ultimately transferred from E2-Nedd8 to specific substrates. The best-known substrates for neddylation are members of the cullin family, which are involved in the assembly of cullin-RING E3 ubiquitin ligases (CRLs). CRLs act as a large family of ubiquitin ligases that regulate cellular protein substrates for proteasomal degradation. The inhibition of the neddylation pathway inactivates CRLs and decreases the protein levels of ubiquitination and subsequent degradation of substrates that are regulated by CRLs substrates, such as Wee1 [13], p27 [14], and Nrf2 [15], leading to the suppression of tumor growth. In recent years, many studies, including our studies, have shown that the level of neddylation enzymes are higher in various types of human cancers compared to adjacent normal tissues [16–20], providing a sound rationale as an attractive cancer treatment strategy. Accumulated experimental data have clearly demonstrated that the overexpression of neddylation enzymes is associated with disease progression, conferring a worse overall patient survival [13,16,17]. Thus, targeting the neddylation pathway is an effective approach to suppressing tumor growth [21–23].

In fact, the potential of NAE as a target in the development of novel anti-cancer therapeutics recently received attention (Fig. 1B). A terminal sulfonamide-based compound, pevonedistat (MLN4924), represents a potentially covalent NAE inhibitor that

conferred significant antitumor activity in phase II/III clinical trials [24]. However, recent preclinical studies identified the resistance to MLN4924 for heterozygous mutations nearby its covalently binding site with NAE, suggesting the development of covalent NAE inhibitors is possibly limited in practice [25,26]. For the R&D of noncovalent neddylation inhibitors, Lu et al. developed a series of piperidin-4-amine scaffold neddylation inhibitors that presented submicromolar NAE inhibitory activities in enzyme-based assays [27,28]. Leung et al. and partners reported serial studies on the discovery of neddylation inhibitors by virtual screening [29–33]. In addition, several series of DCN1 inhibitors have been discovered by high throughput screening (HTS) in recent years [34–39]. However, the small molecule inhibitors mentioned above (except MLN4924) are in preclinical research; thus, there is an urgent need to develop novel inhibitors with better druggability.

CDC (01), as an FDA-approved antihypertensive agent, is converted into candesartan via the first-pass effect of the gastrointestinal tract in the body to play an antihypertensive effect, but we have revealed in a previous study that candesartan has no neddylation inhibitory activity, and CDC is capable of blocking the neddylation pathway of various types of cancers by inhibiting NAE [40]. Although it has moderate neddylation inhibition and anticancer activity, nonoral administration due to its prodrug structure has limited the further development of CDC. In this study, novel CDC-derived neddylation inhibitors were designed and synthesized to promote the neddylation inhibition and overcome the disadvantages of anticancer activities and oral administration of CDC.

## 2. Results and discussion

### 2.1. Design and synthesis

To improve the neddylation inhibitory activity and anticancer efficacy of the lead compound CDC and obtain a novel structural scaffold, chemical modifications were performed in three cycles in this study (Fig. 2). We divided the structure of CDC into three functional regions, namely, regions A, B and C. In our previous work, we showed that region C is a key pharmacophore domain for regulating the neddylation inhibitory activity by comparing with other FDA-approved A2T1R antagonists (structural analogs of CDC) [40]. Hence, based on the strategy of scaffold hopping, we first opened the ring of the benzimidazole in region A and changed the substitution position of the cilexetil group to generate derivatives 5–8 (Table 1). The tetrazole group of CDC was then replaced with various steric substituents in region B to generate derivatives 9–11. Subsequently, comprehensive modifications of the side linker (cilexetil group) in region C aimed to elevate the inhibitory activities and reverse the easy hydrolysis by oral administration of CDC.

The synthetic routes for the preparation of derivatives 5–8 are outlined in Scheme 1. Intermediate 5a was first obtained by a cyclization reaction of 2,3-diaminobenzoic acid and tetraethyl orthocarbonate (commercially available), followed by a nucleophilic substitution reaction with *N*-(triphenylmethyl)-5-(4'-bromomethylbiphenyl-2-yl)tetrazole to yield intermediate 5b. Finally, intermediate 5b was hydrolyzed with 20% trifluoroacetic acid to give target derivative 5. Methyl anthranilate (commercially available) was reacted with butyryl chloride to obtain a mono-substituted amide, which was directly input into the next step without purification to generate intermediate 6a, followed by the nucleophilic substitution of 1-chloroethylcyclohexyl carbonate under the conditions of NaHCO<sub>3</sub>/DMF to generate intermediate 6b; we finally achieved 6 by 20% trifluoroacetic acid hydrolysis. Intermediate 7a was first obtained by a cyclization reaction of methyl 3,4-diaminobenzoate and tetraethyl orthocarbonate. Next, the key intermediate 7b (6-substituted) and its isomer 8b (5-substituted) were achieved by 7a reacting with *N*-(triphenylmethyl)-5-(4'-bromomethylbiphenyl-2-yl)tetrazole under the conditions of K<sub>2</sub>CO<sub>3</sub>/DMF separation and purification by silica gel column chromatography. Intermediates 7b and 8b were hydrolyzed under lithium hydroxide to obtain their carboxylates, and the crude products were directly reacted with 1-chloroethylcyclohexyl carbonate to obtain intermediates 7c and 8c. Intermediate 7c and 8c were deprotected under 20% trifluoroacetic acid conditions to obtain the target compounds 7 and 8.

Derivatives 9–46 were prepared as described in Scheme 2. Derivatives 9 and 10 were prepared by using similar synthetic routes as those of 7 or 8. Analog 11 was achieved by methylation of CDC. Candesartan reacts with triphenylmethyl bromide to obtain intermediate 12a, which was then condensed with various substituted amines; finally, trifluoroacetic acid was hydrolyzed to produce derivatives 12–46.

### 2.2. In vitro biological evaluations

#### 2.2.1. Preliminary investigation of neddylation inhibitory activities and anti-proliferation abilities of benzimidazole derivatives

Cullins act as one of the most important neddylation substrates that can accurately reflect the level of Nedd8 modification in cancer cells, while the formation of cullin1-Nedd8 adduct was explored as a critical indicator for investigating the inhibitory activities of derivatives rationally [5,6]. Initial studies involved in the investigation of structurally modified derivatives in region A and region B were performed by exploring the levels of cullin1-Nedd8 adduct at the enzyme-based assay, along with anti-proliferation activities on A549 human lung cancer cells. As shown in Table 1, we first tried to replace benzimidazole (region A) with ring-opening (6), resulting in the reduced neddylation inhibitory activity of the derivatives. Next, we replaced, removed or methylated the tetrazolium group to obtain derivatives 9–11. Unfortunately, they have poorer neddylation inhibitory activity compared to CDC.

In comparison with lead compound CDC, removal of the cilexetil group (5) in region C and replacement of the cilexetil group with 5 (8) and 6 (7) substitutions leads to a decrease in neddylation inhibitory activity. Perhaps the presence of cilexetil groups and the 7-position substitution are important for maintaining the neddylation inhibition of the derivatives. Combined with the results of molecular docking in our previous study, we preliminarily speculate that regions A and B are groups that maintain neddylation inhibitory activity. Thus, to keep it unchanged, we turned our attention to region C. As is known, the cilexetil group has emerged as a prodrug group that is vulnerable upon oral administration. In addition, CDC has poor water solubility, and its water solubility can be improved by replacing ester bonds with amide bonds to increase stability.

Next, we focused on the systemic variation in region C for stabilizing the structure and elevating the inhibitory activities and water solubility of the new derivatives. As shown in Table 2, the cilexetil group was replaced with an aliphatic chain or an aliphatic ring to obtain a series of derivatives, 12–20, but the neddylation inhibitory activity was reduced to varying degrees compared to that

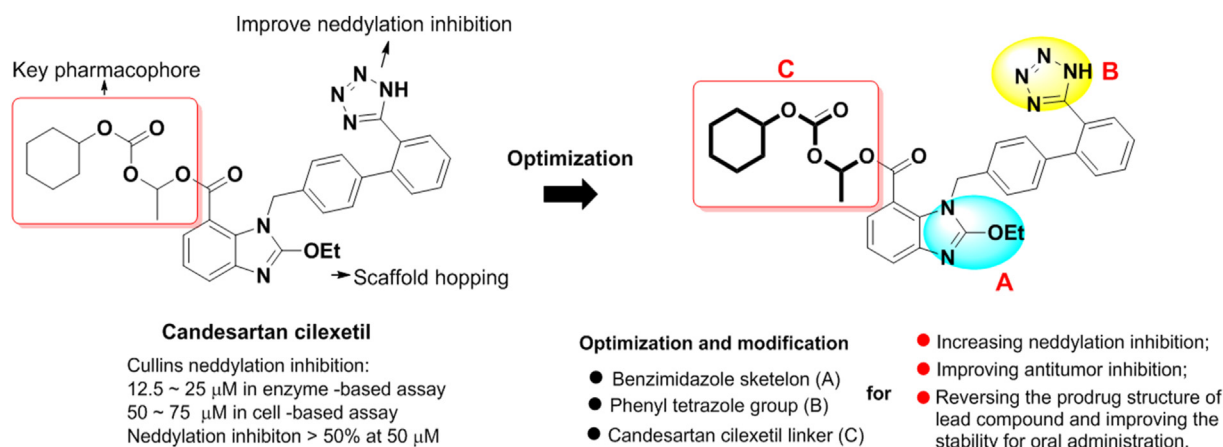
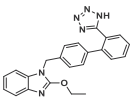
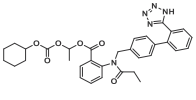
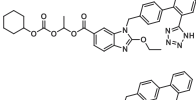
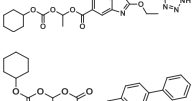
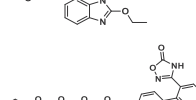
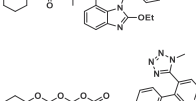
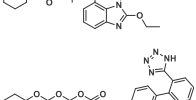
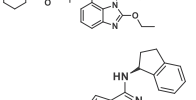
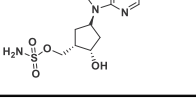


Fig. 2. Chemical optimization strategies and purposes for lead compound CDC.

**Table 1**  
Neddylaton inhibition in enzyme-based assay and the antitumor activities against A549 human lung cancer cells of derivatives 5–11.

Compd.	Structure	Cullin1-Nedd8 inhibition % @ 25 $\mu\text{M}^{\text{a}}$	A549 inhibition% @ 100 $\mu\text{M}^{\text{b}}$
5		18.9%	9.5%
6		32.6%	15.2%
7		43.2%	56.9%
8		44.7%	33.3%
9		29.5%	34.2%
10		34.2%	14.6%
11		41.2%	16.8%
CDC (01)		87.8%	69.2%
MLN4924		90.5%	91.4%

<sup>a</sup> The neddylaton rate of cullin1-Nedd8 in enzyme-based assay and are reported as the average of three experiments.

<sup>b</sup> The *anti*-proliferation rate in A549 and are reported as the average of three experiments.

of CDC. Considering that the NAE pocket is relatively flat, a series of aromatic ring-substituted derivatives were synthesized (**21–37**). The replacement of the cilexetil group with phenylethylamine led to the superior inhibition of derivatives, such as **33** and **35**. According to the results, more terminal phenethylamine derivatives were designed and synthesized to evaluate the neddylaton and proliferation inhibitory activities (Table 3, Fig. 2), some of which (**39**, **46**) displayed superior efficacy than the lead compound CDC.

### 2.2.2. Structure-activity relationships (SARs)

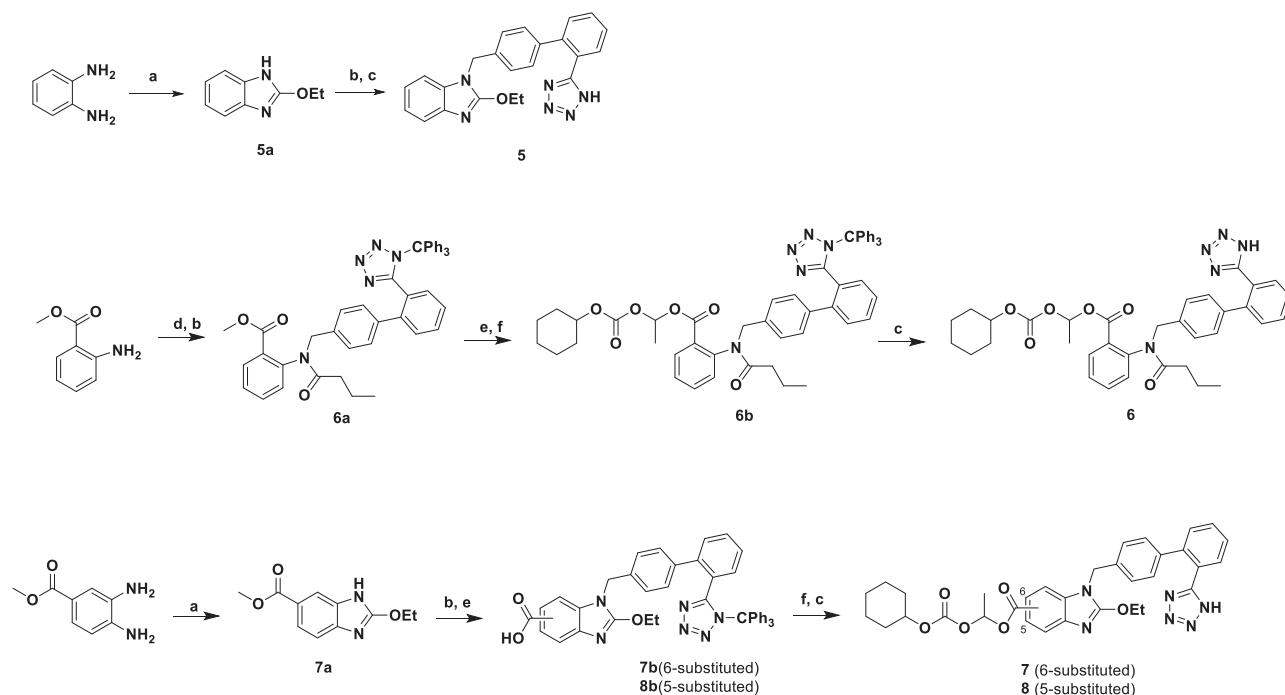
According to the structural features and the preliminary results of the neddylaton inhibitory abilities and anti-proliferation activities of the derivatives, the SARs are summarized in detail. (1) The scaffolds of benzimidazole and tetrazole groups are important for improving the neddylaton inhibitory activities of the derivatives (**1** vs. **5–10**). (2) The replacements of the substituents of (cyclo) alkyl, benzoalicyclic and heterocyclic groups into region C are unfavorable for the neddylaton inhibitory activities of the derivatives (**24**, **33** vs. **12–20**, **25–27**), while the replacement of phenyl groups is beneficial for those of the derivatives. (3) The introduction of electron-withdrawing groups or halogen atoms into the phenyl rings increased more neddylaton inhibition than that of the

electron-donating ones (**22**, **24**, **33–35** vs **23**, **27**, **31**). (4) Substitutions at the phenyl ring by chlorine atoms presented superior efficacy over other groups, while the substitution at the para-position provided significant improvements in activities (**35**, **39**, **46** vs. **38**, **40–45**).

### 2.2.3. Optimal compounds suppress the growth of cancer cell by inhibiting the neddylaton pathway

Next, derivatives **35**, **39** and **46** as the optimal compounds were selected for investigating neddylaton inhibitory activities and cellular anti-proliferation abilities at various concentrations with either two human lung cancer cell lines (A549 and H1299) or two human normal cell lines (16H6E and BEAS-2E), as shown in Table 4. The results showed that three derivatives displayed excellent inhibitory activities on the formation of cullin1-Nedd8 adducts at the micromolar concentration in the enzyme-based assay, along with selectively inhibiting the proliferation of cancer cells without affecting the normal ones. In general, derivative **35** presented superior neddylaton inhibitory activities and anticancer selectivity.

In light of the inhibitory activity of the cullin1-Nedd8 adduct and selective anti-proliferation activities in cancer cells, derivative **35** was chosen to further investigate the neddylaton inhibition in



**Scheme 1.** Synthesis of Compounds **5-8**<sup>a</sup>

<sup>a</sup>Reagents and conditions: (a) C(OEt)<sub>4</sub>, AcOH, 0 °C to rt, 4 h, 90%; (b) *N*-(triphenylmethyl)-5-(4'-bromomethylbiphenyl-2-yl)tetrazole, K<sub>2</sub>CO<sub>3</sub>, DMF, 60 °C, overnight, 45%; (c) 20% trifluoroacetic acid in dichloromethane, rt, 4 h, 90%; (d) Butyryl chloride, DIPEA, dichloromethane, reflux, overnight, 90%; (e) LiOH·H<sub>2</sub>O, 5eq, MeOH:H<sub>2</sub>O = 1:1, reflux, 6 h; (f) 1-chloroethyl cyclohexyl carbonate, NaHCO<sub>3</sub>, NaI, DMF, 60 °C, overnight, 40%.

the cell-based assay. Cullin family members act as the best-known substrates of neddylation that are involved in the assembly of CRLs, which also represent a significant index for evaluating the neddylation inhibitory activities of inhibitors. Furthermore, in the process of cullin neddylation, individual cullins 1, 2, 3, 4a/b are specially regulated by Nedd8 conjugating enzyme Ubc12, while cullin 5 is controlled by another Nedd8 conjugating enzyme UBE2F. In addition, when the upstream Nedd8 activating enzyme, NAE, is blocked, the entire cullin-Nedd8 adduct will be inhibited (Fig. 3A). According to the principle described above, our previous work demonstrated that lead compound CDC can inhibit the formation of the cullin-Nedd8 adduct by targeting NAE. We continuously verified the specific target of representative **35** by utilizing these methods.

Herein, the levels of various cullin-Nedd8 (cullins 1, 2, 4a, 5) adducts were first examined by immunoblotting after the treatment of **35** in A549 (Fig. 3B). In general, **35** acted as an efficient neddylation inhibitor for suppressing the entire cullins neddylation significantly at 12.5–25 μM, which also displayed significant effects compared with lead compound CDC upon comparison with MLN4924. Furthermore, the results of cullins and enzyme UBE2M (E2) neddylation inhibition suggested that **35** inhibited neddylation by targeting the NAE enzyme in the mechanism, similar to CDC. The level of global protein neddylation was explored in parallel with the displayed significant decline with the increase in concentration of **35**, which further indicated that **35** inhibited NAE. Meanwhile, two representative CRL substrates, Wee1 and p27, accumulated obviously after treatment with **35** at the concentration of 50 μM (Fig. 3C), validating that **35** stabilized the CRL substrates by suppressing the neddylation-CRL pathway.

Accumulated studies showed that blocking the neddylation pathway induces cell death via apoptosis. The result in Fig. 3B showed that the apoptosis-related marker cleaved-PARP was accumulated by the treatment of **35** at the concentration of 12.5 μM in A549, which preliminarily indicates that **35** induced cellular

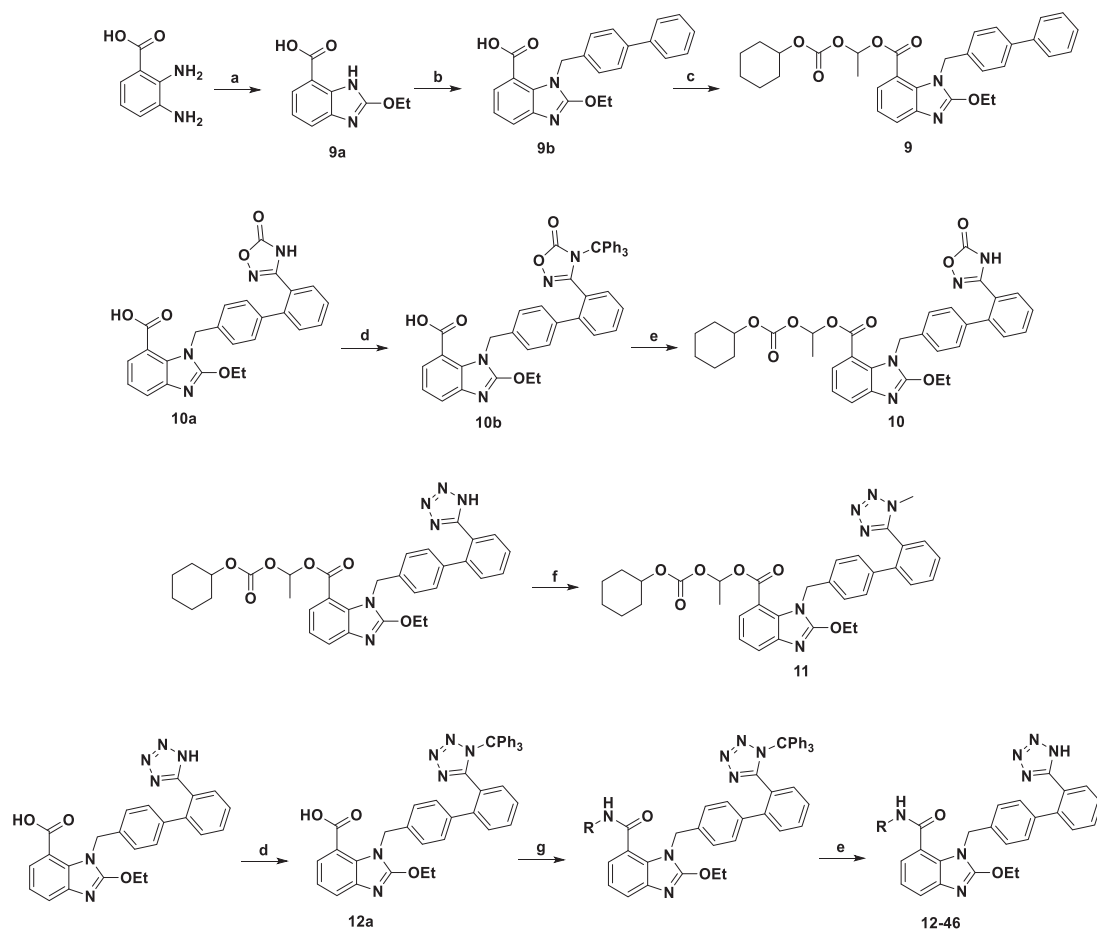
apoptosis. As shown in Fig. 4A, an annexin-V/PI double staining assay was performed to further assess the ability of derivative **35** to induce apoptosis. The results showed that the total ratio of early and late apoptotic A549 cells increased from 2.6% to 35.81% with increasing concentrations of **35**, suggesting that **35** induced cancer cell apoptosis. Besides, considering that targeting the neddylation pathway usually induces cellular senescence. As shown in Fig. 4B, an SA-β-gal staining assay was performed to assess the ability of derivative **35** to induce senescence. The results demonstrated **35** treatment promoted the senescence of lung cancer cell at the concentration of 10 μM, indicating that compound **35** can induce cellular senescence.

### 2.3. Molecular modeling studies

Our previous work confirmed that lead compound CDC as a novel neddylation inhibitor can bind with the ATP-binding pocket of NAE, as shown by molecular modeling. Similarly, molecular modeling was established to investigate the binding mode of **35** with NAE using Autodock 4.0. As shown in Figs. 4C–1 and 2, **35** was found to form various interactions in the binding pocket, including several H-bonds with the amino acid residues of K124 (2.2 Å), N168 (2.7 Å), Q112 (1.9 Å) and G76 (2.4 Å). Furthermore, the side chain guanidine groups of R22 (3.1 Å) and R111 (3.3 Å) formed two additional π-π conjugations with structural benzimidazole and phenyl groups of derivative **35**, respectively, suggesting that the affinity of **35** with NAE was higher than that of CDC (Figs. 4C–2 and 3).

### 2.4. Neddylation inhibitor **35** suppresses the growth of A549 xenograft tumors in mice

To investigate the anticancer activity of **35** *in vivo*, we administered **35** to nude mice bearing human tumor cell xenografts and



**Scheme 2.** Synthesis of Compounds 9–46<sup>b</sup>

<sup>b</sup>Reagents and conditions: (a) C(OEt)<sub>4</sub>, AcOH, 0 °C to rt, 4 h, 90%; (b) 4-bromomethylbiphenyl-2-yl, K<sub>2</sub>CO<sub>3</sub>, dichloromethane, 60 °C, overnight, 84%; (c) 1-chloroethyl cyclohexyl carbonate, NaHCO<sub>3</sub>, DMF, 60 °C, overnight, 76%; (d) Triphenylmethyl bromide, NEt<sub>3</sub>, dichloromethane, rt, overnight, 85%; (e) 20% trifluoroacetic acid in DCM, rt, 4 h, 90%; (f) CH<sub>3</sub>I, dichloromethane, reflux, overnight, 52%; (g) R–NH<sub>2</sub>, EDCI, HOBT, DIPEA, DMF, overnight, 28–78%.

monitored the tumor growth rate. First,  $2 \times 10^6$  A549 cells in 0.1 mL of PBS were subcutaneously inoculated into female nude mice. After the tumor size reached the requirements (tumor volume of 70–100 mm<sup>3</sup>, approximately 8 days), the tumor-bearing mice were randomly divided into 5 groups (6 mice per group): a mock group, a CDC-treated group as the positive control administered by intraperitoneal injection (30 mg/kg qd), a **35**-treated group administered by intraperitoneal injection (30 mg/kg qd) and two **35**-treated groups by oral administration (60 mg/kg qd or 30 mg/kg qd), (Fig. 5).

As shown in Fig. 5A and B, in contrast to the mock group, three **35**-treated groups showed a significant decrease in tumor volume and tumor weight except for that with oral administration at the dosage of 30 mg/kg qd, while all treated groups showed no effect on body weight after 24 days (Fig. 5A and B). The **35**-treated group with the high dosage (60 mg/kg qd) by oral administration presented significant tumor inhibitory activity, suggesting that the strategy of elevating the stability of derivatives *in vivo* is feasible by modifying the structure of CDC. In addition, the **35**-treated group by intraperitoneal injection (30 mg/kg) displayed superior anticancer activity in comparison with the tumor weight and size of the other treated groups (Fig. 5C and D).

### 3. Conclusion

Our previous work screened 1331 approved drugs from an in-

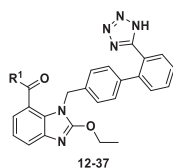
house “old drug bank”, and CDC was discovered as a potential neddylation inhibitor [40]. To overcome the defect of structurally easy hydrolysis and promote the anticancer ability of lead compound CDC, 42 derivatives with a novel benzimidazole skeleton were designed and synthesized through a rational structure-based drug design strategy in this study. Derivative **35** displayed both superior neddylation inhibitory activity and cellular anti-proliferation ability of those of other compounds. Additional annexin-V/PI double staining assays and SA-β-gal staining assay showed that **35** induces apoptosis and promotes senescence in the A549 cancer cells. Antitumor activity *in vivo* indicated that **35** not only suppressed the growth of A549 xenograft tumors in the mice upon administration of intraperitoneal injection (30 mg/kg) but also presented promising efficacy through oral administration (60 mg/kg). In summary, we have discovered a new class of neddylation inhibitors of the benzimidazole scaffold, which can be used as candidate compounds for the development of new anticancer drugs.

## 4. Experimental sections

### 4.1. General methods

The synthetic starting materials, reagents, and solvents were obtained from commercial supplier, such as Alfa Aesar, Adamasbeta, Energy Chemical, J&K, and TCI at the highest commercial

**Table 2**  
Neddylation inhibition in enzyme-based assay and the antitumor activities against A549 human lung cancer cells of derivatives 12–37.

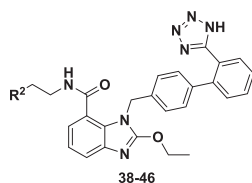


Com pd.	R <sup>1</sup>	Cullin1-Nedd8 inhibition % @ 25 μM <sup>a</sup>	A549 inhibition % @ 100 μM <sup>b</sup>	Com pd.	R <sup>1</sup>	Cullin1-Nedd8 inhibition % @ 25 μM <sup>a</sup>	A549 inhibition % @ 100 μM <sup>b</sup>
12		32.6 %	12.5 %	25		39.8 %	39.5 %
13		30.9 %	11.3 %	26		37.5 %	18.9 %
14		39.7 %	11.9 %	27		34.9 %	16.7 %
15		36.8 %	12.1 %	28		48.9 %	54.5 %
16		29.5 %	9.8 %	29		38.1 %	35.4 %
17		27.9 %	10.1 %	30		35.7 %	31.6 %
18		29.4 %	11.2 %	31		47.9 %	53.19 %
19		46.5 %	32.7 %	32		39.4 %	43.8 %
20		28.6 %	9.2 %	33		66.1 %	51.4 %
21		34.6 %	13.1 %	34		47.5 %	53.5 %
22		45.3 %	66.3 %	35		86.4 %	83.9 %
23		25.8 %	10.5 %	36		39.8 %	24.3 %
24		60.9 %	54.4 %	37		64.6 %	< 20 %

<sup>a</sup>The neddylation rate of cullin1-Nedd8 in enzyme-based assay and are reported as the average of three experiments. <sup>b</sup>The anti-proliferation rate in A549 and are reported as the average of three experiments.

quality and used without further purification. Reaction progress was monitored using analytical thin layer chromatography (TLC), HSGF 254 (150–200 μm thickness; Yantai Huiyou Co.; China), UV light (254 nm) and I<sub>2</sub> were used to visualize the components. Melting points were measured in capillary tubes on a SGWX-4 melting point apparatus without correction. <sup>1</sup>H NMR and <sup>13</sup>C NMR spectra were recorded on a Bruker AMX 400 and AMX 500 spectrometer in DMSO-*d*<sub>6</sub>, MeOD-*d*<sub>4</sub> or CDCl<sub>3</sub> with TMS as internal

standard. Chemical shifts were reported in parts per million (ppm, δ) downfield from tetramethylsilane. Proton coupling patterns were described as singlet (s), doublet (d), triplet (t), quartet (q), and multiplet (m). High-resolution mass spectra (HRMS) were obtained by electric ionization (EI) and electrospray ionization (ESI) using a Waters GCT Premie and XEVO-G2TOF<sup>1</sup> NotSet. All target compounds were purified to ≥95% purity as determined by an Agilent 1100 with a quaternary pump and diode array detector (DAD).

**Table 3**Neddylation inhibition in enzyme-based assay and the antitumor activities against A549 human lung cancer cells of derivatives **38–46**.

Compd.	R <sup>2</sup>	Cullin1-Nedd8 inhibition % @ 25 μM <sup>a</sup>	A549 inhibition% @ 100 μM <sup>b</sup>	Compd.	R <sup>2</sup>	Cullin1-Nedd8 inhibition % @ 25 μM <sup>a</sup>	A549 inhibition% @ 100 μM <sup>b</sup>
<b>38</b>		86.69 %	45.5 %	<b>43</b>		57.43 %	36.6%
<b>39</b>		82.86 %	77.6 %	<b>44</b>		47.6 %	36.2 %
<b>40</b>		43.6 %	57.7%	<b>45</b>		35.8 %	12.5 %
<b>41</b>		32.1 %	15.7 %	<b>46</b>		74.66 %	71.6 %
<b>42</b>		35.7 %	14.2 %				

<sup>a</sup>The neddylation rate of cullin1-Nedd8 in enzyme-based assay and are reported as the average of three experiments. <sup>b</sup>The anti-proliferation rate in A549 and are reported as the average of three experiments.

**Table 4**The inhibitory activities of selected compounds **35**, **39** and **46** on the formation of cullin1-Nedd8 adducts, the proliferation of Human lung cancer cell lines (A549, H1299) and human normal cell lines (16H6E, BEAS-2B).<sup>a</sup>

Compd.	Cullin1-Nedd8 inhibition (IC <sub>50</sub> , μM)	Anti-proliferative activity (IC <sub>50</sub> , μM)			
		A549	H1299	16H6E	BEAS-2B
<b>35</b>	5.51 ± 0.33	20.39 ± 1.47	21.76 ± 2.7	76.06 ± 2.43	79.35 ± 1.89
<b>39</b>	6.67 ± 0.32	39.29 ± 1.37	36.74 ± 1.01	64.91 ± 3.82	80.84 ± 3.10
<b>46</b>	9.94 ± 0.41	19.12 ± 1.09	18.25 ± 1.53	44.7 ± 1.21	37.91 ± 2.59
CDC	16.43 ± 0.12	65.92 ± 1.63	45.02 ± 1.55	82.67 ± 2.22	79.76 ± 1.90
MLN4924	0.18 ± 0.02	0.63 ± 0.06	0.49 ± 0.04	4.03 ± 0.07	1.22 ± 0.1

<sup>a</sup> The values are reported as the average ± SD of three experiments.

## 4.2. Synthesis of intermediates and target compounds **5–11**

### 4.2.1. 2-Ethoxy-1H-benzo[d]imidazole (**5a**)

The compound benzene-1,2-diamine (0.56 g, 3.68 mmol) and acetic acid (20 mL) were added to a round bottom flask. After mixing, tetraethyl orthocarbonate (0.9 mL, 4.30 mmol) was slowly added dropwise to the system under ice bath conditions, stirring was continued under ice bath conditions, and reacted at room temperature for 4 h. After the reaction was completed, the reaction solution was poured into an ice water bath. Brown solid, yield 88%. <sup>1</sup>H NMR (400 MHz, CDCl<sub>3</sub>) δ 9.56 (s, 1H), 7.51–7.32 (m, 2H), 7.23–7.00 (m, 2H), 4.58 (q, *J* = 7.1 Hz, 2H), 1.44 (t, *J* = 7.1 Hz, 3H).

### 4.2.2. 1-((2'-((1H-tetrazol-5-yl)-[1,1'-biphenyl]-4-yl)methyl)-2-ethoxy-1H benzo[d]imidazole (**5**)

In a 50 mL round-bottomed flask, add intermediates **5a** (0.13 g, 0.5 mmol), K<sub>2</sub>CO<sub>3</sub> (0.1 g, 0.75 mmol) in DMF (4 mL). Then *N*-(triphenylmethyl)-5-(4'-bromomethylbiphenyl-2-yl)-terazole (0.28 g, 0.5 mmol) was added after stirring at room temperature for 10 min. After 60 °C overnight reaction, when the reaction was completed, the reaction solution was poured into an ice water bath, diluted with EtOAc and washed with distilled water, followed by brine. The organic layer was dried (MgSO<sub>4</sub>), filtered and concentrated in vacuo to give the desired intermediates without further purification.

Intermediate was added to the round bottom flask, then a DCM solution (4 mL) containing 20% trifluoroacetic acid was added

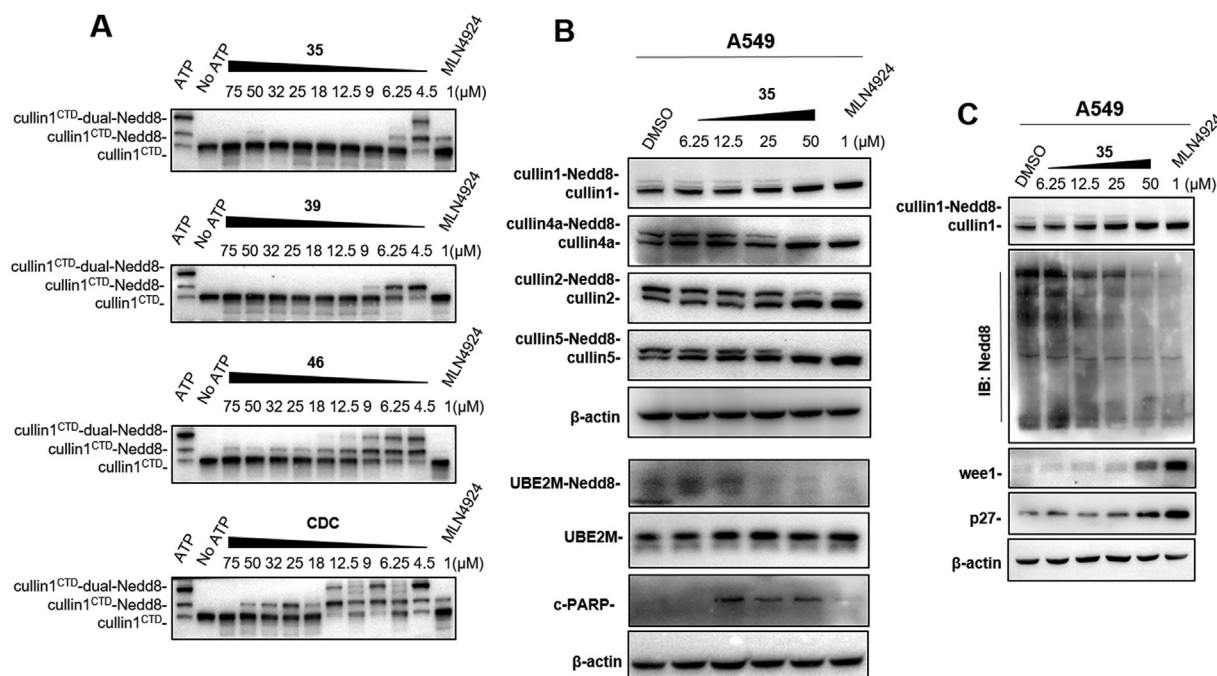


**Fig. 3.** Analog **35** is an NAE inhibitor. (A) The cullin1-Nedd8 inhibitory activities of optimal **35**, **39**, **46** and CDC. (B) **35** inhibited global neddylation and induced the accumulation of apoptosis marker cleaved-parp in human lung A549 cancer cell line. (C) **35** inhibited cullins neddylation and CRL substrates degradation in A549 cancer cell line.

dropwise under ice bath conditions. After 4 h of reaction at room temperature, the solvent was removed by rotary evaporation, neutralized to neutral in  $\text{NaHCO}_3$  solution, EtOAc was extracted ( $3 \times 50$  mL), followed by brine. The organic layer was dried ( $\text{MgSO}_4$ ), filtered and concentrated in vacuo to give the desired crude product. After separation and purification by silica gel column chromatography to give the white solid compound **5**. White solid, yield 35%, mp = 170–172 °C.  $^1\text{H}$  NMR (400 MHz,  $\text{DMSO}-d_6$ )  $\delta$  12.35 (s, 1H), 7.68–7.58 (m, 2H), 7.58–7.52 (m, 2H), 7.32 (t,  $J = 7.7$  Hz, 2H), 7.27 (d,  $J = 7.2$  Hz, 2H), 7.01 (d,  $J = 8.5$  Hz, 1H), 6.90 (d,  $J = 8.1$  Hz, 1H), 6.80 (d,  $J = 8.1$  Hz, 1H), 5.35 (s, 2H), 4.68–4.54 (m, 1H), 1.40 (dd,  $J = 13.6, 6.6$  Hz, 3H).

#### 4.2.3. Methyl 2-(*N*-((2'-(1-trityl-1*H*-tetrazol-5-yl)-[1,1'-biphenyl]-4-yl)methyl)butyramido)benzoate (**6a**)

In a round bottom flask was added the compound methyl anthranilate (0.75 g, 5 mmol), DIPEA (2.6 mL, 15 mmol) was dissolved in DCM (20 mL), and stirred at room temperature for 10 min, then add butyryl chloride (1.5 mL, 15 mmol). The reaction mixture was stirred and refluxed overnight. After the reaction was completed, the crude product is obtained by water quenching, dichloromethane extraction, vacuum evaporation and solvent removal. The crude product was directly subjected to the next reaction without purification.

To a round bottom flask was added corresponding intermediate (0.08 g, 0.5 mmol),  $\text{K}_2\text{CO}_3$  (0.07 g, 0.6 mmol), DMF (2 mL), and stirred at room temperature for 10 min, then add *N*-(triphenylmethyl)-5-(4'-bromomethylbiphenyl-2-yl)terazole (0.28 g, 0.5 mmol), then 60 °C overnight reaction. After the reaction was completed, the reaction mixture was poured into an ice water bath, EtOAc was extracted ( $3 \times 50$  mL), followed by brine. The organic layer was dried ( $\text{MgSO}_4$ ), filtered and concentrated in vacuo to give the desired crude product, which was purified by silica gel column chromatography to obtain the corresponding intermediate **6a** (0.19 g, 62%).

#### 4.2.4. 1-(((cyclohexyloxy)carbonyloxy)ethyl 2-(*N*-((2'-(1-trityl-1*H*-tetrazol-5-yl)-[1,1'-biphenyl]-4-yl)methyl)butyramido)benzoate (**6b**)

The intermediate **6a** (0.80 g, 1.16 mmol) was added to a solution of the  $\text{LiOH} \cdot \text{H}_2\text{O}$  (5 mL) in MeOH/ $\text{H}_2\text{O}$  mixture (4 mL, MeOH:  $\text{H}_2\text{O} = 1:1$ ) at room temperature and stirred at 80 °C in air. After 6 h, the reaction was cooled to room temperature, diluted with EtOAc and washed with distilled water, followed by brine. The organic layer was dried ( $\text{MgSO}_4$ ), filtered and concentrated in vacuo to give the desired carboxylate intermediates without further purification.

The carboxylate intermediates (0.51 g, 0.6 mmol), 1-chloroethyl cyclohexyl carbonate (0.15 g, 0.72 mmol),  $\text{NaHCO}_3$  (0.08 g, 0.9 mmol), NaI (0.01 g, 0.09 mmol), DMF (5 mL) were added to the round-bottom flask. After 60 °C reaction overnight, the reaction liquid was poured into ice water bath, diluted with EtOAc and washed with distilled water, followed by brine. The organic layer was dried ( $\text{MgSO}_4$ ), filtered and decompressed to remove solvents. The crude products were separated and purified by silica gel column chromatography, and the corresponding intermediates **6b** were obtained.

#### 4.2.5. 1-(((cyclohexyloxy)carbonyloxy)ethyl 2-(*N*-((2'-(1*H*-tetrazol-5-yl)-[1,1'-biphenyl]-4-yl)methyl)butyramido)benzoate (**6**)

Compound **6** was synthesized according to a similar protocol as that described for **5**. White solid, yield 52%, mp = 172–175 °C.  $^1\text{H}$  NMR (400 MHz,  $\text{MeOD}-d_4$ )  $\delta$  8.04 (t,  $J = 7.3$  Hz, 1H), 7.74–7.66 (m, 2H), 7.65–7.47 (m, 4H), 7.12 (d,  $J = 7.8$  Hz, 2H), 7.04 (d,  $J = 7.9$  Hz, 2H), 6.98–6.88 (m, 1H), 6.82 (d,  $J = 7.8$  Hz, 1H), 5.61 (dd,  $J = 14.5, 9.5$  Hz, 1H), 4.72–4.59 (m, 1H), 4.07–3.95 (m, 1H), 2.03–1.96 (m, 2H), 1.92 (s, 2H), 1.75 (s, 2H), 1.64–1.38 (m, 11H), 0.84 (t,  $J = 7.4$  Hz, 3H). HRMS (ESI)  $m/z$  calcd  $\text{C}_{34}\text{H}_{37}\text{N}_5\text{O}_6$   $[\text{M}+\text{Na}]^+$  634.2642, found 634.2640.

#### 4.2.6. Methyl 2-ethoxy-1*H*-benzo[d]imidazole-6-carboxylate (**7a**)

Compound **7a** was synthesized according to a similar protocol as

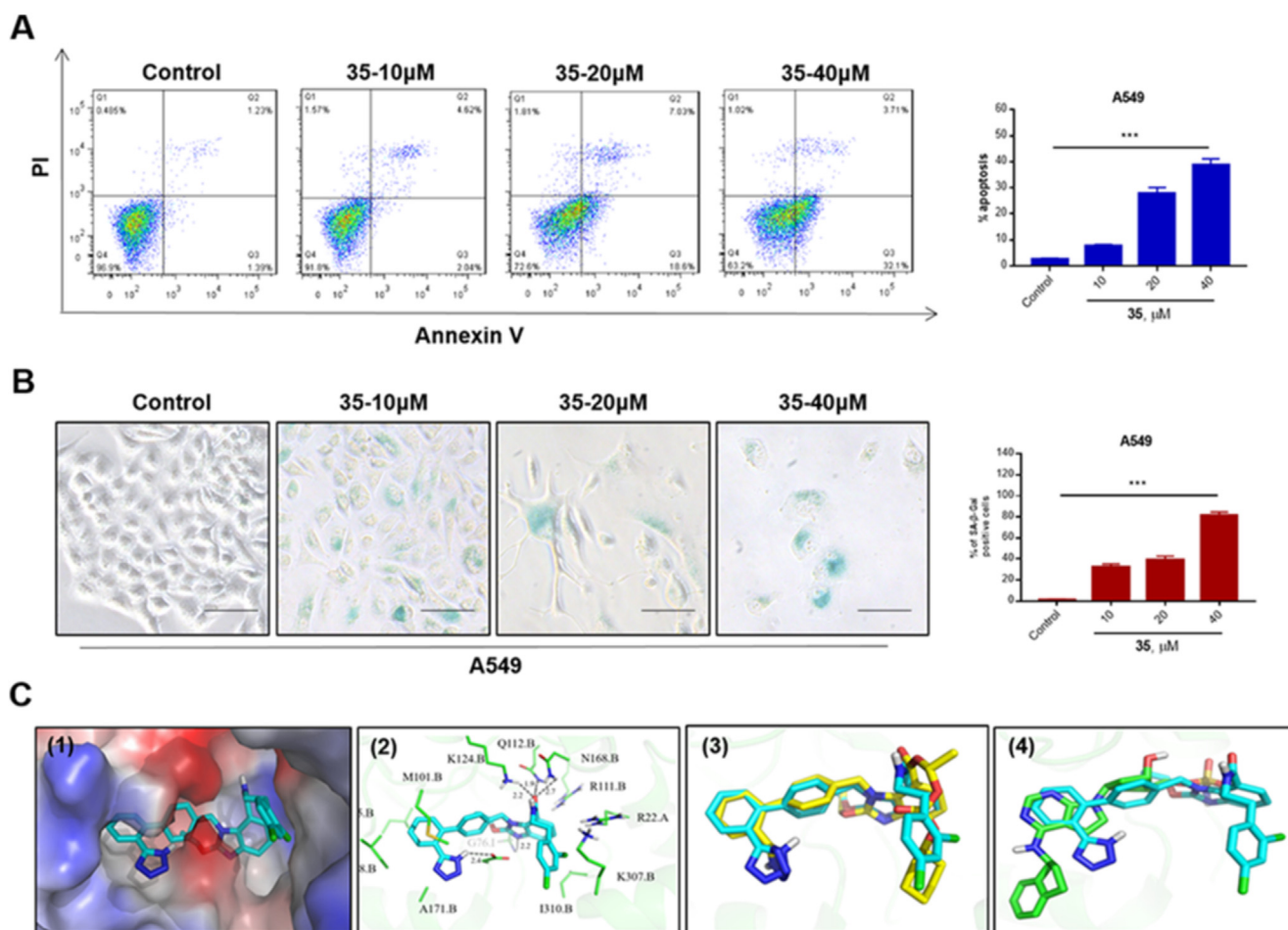


**Fig. 4.** **35** induces the apoptosis and promotes senescence of lung cancer cell A549 by the target of enzyme NAE. (A) Evaluation of apoptosis on A549 cell line by Annexin V/PI staining and flow cytometry detecting. 0.1% DMSO treated A549 cells in 48 h; **35** treated A549 cells in 48 h at the concentration of 10, 20, or 40  $\mu\text{M}$ . (B) **35** treatment promotes the senescence of lung cancer cell lines A549 by SA- $\beta$ -gal staining; scale bar: 50  $\mu\text{m}$ . (C) Molecular modeling results (PDB ID: 3GZLN): (1) Low-energy binding conformations of **35** (shown in blue) bound to NAE heterodimer generated by virtual ligand docking; (2) The hydrogen-bonding interaction between the structure of **35** with NAE; (3) Merging between **35** pose (shown in blue) and CDC conformation (shown in yellow) from NAE crystal. (4) Merging between **35** pose (shown in blue) and MLN4924 conformation (shown in green) from NAE crystal. Statistical significance was determined by the Mann-Whitney test (two-tailed): \*\*\* $p < 0.001$ . (For interpretation of the references to colour in this figure legend, the reader is referred to the Web version of this article.)

that described for **5a**. White solid, yield 87%,  $^1\text{H}$  NMR (400 MHz,  $\text{CDCl}_3$ ) 7.53–7.30 (m, 2H), 7.27–7.05 (m, 2H), 4.68 (q,  $J = 7.1$  Hz, 2H), 3.89 (s, 3H), 1.29 (t,  $J = 7.1$  Hz, 3H).

#### 4.2.7. 2-Ethoxy-1-((2'-(1-trityl-1H-tetrazol-5-yl)-[1,1'-biphenyl]-4-yl)methyl)-1H-benzo[d]imidazole-5-carboxylic acid (**7b**)

The intermediate **7b** (0.13 g, 0.5 mmol) was added to a solution of the  $\text{K}_2\text{CO}_3$  (0.1 g, 0.75 mmol) in DMF (4 mL) at room temperature, then *N*-(triphenylmethyl)-5-(4'-bromomethylbiphenyl-2-yl)-terazole (0.28 g, 0.50 mmol) was added after stirring at room temperature for 10 min. Finally, stirred at 60  $^\circ\text{C}$  overnight reaction in air. After 6 h, the reaction was cooled to room temperature, diluted with EtOAc and washed with distilled water, followed by brine. The organic layer was dried ( $\text{MgSO}_4$ ), after the solvent was evaporated in vacuo, the residue was purified by flash column chromatography ( $\text{CHCl}_3$ -EtOAc = 20:1). The first eluate was concentrated in vacuo to give **7b**. White solid, yield 37%. Intermediate **7b**:  $^1\text{H}$  NMR (400 MHz,  $\text{DMSO}-d_6$ )  $\delta$  12.74 (s, 1H), 7.77 (dd,  $J = 7.6, 1.3$  Hz, 1H), 7.68 (dd,  $J = 7.9, 1.0$  Hz, 1H), 7.55–7.46 (m, 3H), 7.38 (dd,  $J = 12.6, 6.7$  Hz, 5H), 7.31 (t,  $J = 7.4$  Hz, 5H), 7.31–7.08 (m, 1H), 6.97 (d,  $J = 8.2$  Hz, 2H), 6.96–6.64 (m, 8H), 5.34 (s, 2H), 4.43 (q,  $J = 7.1$  Hz, 2H), 1.35 (t,  $J = 7.1$  Hz, 3H). and the second eluate was concentrated in vacuo to give **8b** [41].

#### 4.2.8. 1-(((cyclohexyloxy)carbonyloxy)ethyl 1-((2'-(1H-tetrazol-5-yl)-[1,1'-biphenyl]-4-yl)methyl)-2-ethoxy-1H-benzo[d]imidazole-6-carboxylate (**7**)

Compound **7** was synthesized according to a similar protocol as that described for **5**. White solid, yield 42%, mp = 171–175  $^\circ\text{C}$ .  $^1\text{H}$  NMR (400 MHz,  $\text{DMSO}-d_6$ )  $\delta$  7.99 (s, 1H), 7.73 (d,  $J = 8.2$  Hz, 2H), 7.65–7.57 (m, 3H), 7.51 (d,  $J = 8.3$  Hz, 1H), 7.20 (d,  $J = 8.2$  Hz, 2H), 7.03 (d,  $J = 8.2$  Hz, 2H), 6.89–6.84 (m, 1H), 6.08 (s, 1H), 5.29 (s, 2H), 4.60–4.55 (m, 2H), 4.10 (dd,  $J = 10.5, 5.2$  Hz, 1H), 1.81 (s, 3H), 1.70–1.45 (m, 10H), 1.38 (s,  $J = 7.1$  Hz, 3H). HRMS (ESI)  $m/z$  calcd  $\text{C}_{33}\text{H}_{34}\text{N}_6\text{O}_6$   $[\text{M}+\text{H}]^+$  611.2618, found 611.2619.

#### 4.2.9. 1-(((cyclohexyloxy)carbonyloxy)ethyl 2-ethoxy-1-((2'-(1-trityl-1H-tetrazol-5-yl)-[1,1'-biphenyl]-4-yl)methyl)-1H-benzo[d]imidazole-5-carboxylate (**8**)

Compound **8** was synthesized according to a similar protocol as that described for **5**. White solid, yield 35%, mp = 172–175  $^\circ\text{C}$ .  $^1\text{H}$  NMR (400 MHz,  $\text{DMSO}-d_6$ )  $\delta$  7.99 (s, 1H), 7.73 (d,  $J = 8.2$  Hz, 2H), 7.65–7.57 (m, 3H), 7.51 (d,  $J = 8.3$  Hz, 1H), 7.20 (d,  $J = 8.2$  Hz, 2H), 7.03 (d,  $J = 8.2$  Hz, 2H), 6.89–6.84 (m, 1H), 6.08 (s, 1H), 5.29 (s, 2H), 4.60–4.55 (m, 2H), 4.10 (dd,  $J = 10.5, 5.2$  Hz, 1H), 1.81 (s, 3H), 1.70–1.45 (m, 10H), 1.38 (s,  $J = 7.1$  Hz, 3H). HRMS (ESI)  $m/z$  calcd  $\text{C}_{33}\text{H}_{34}\text{N}_6\text{O}_6$   $[\text{M}+\text{H}]^+$  611.2618, found 611.2615.

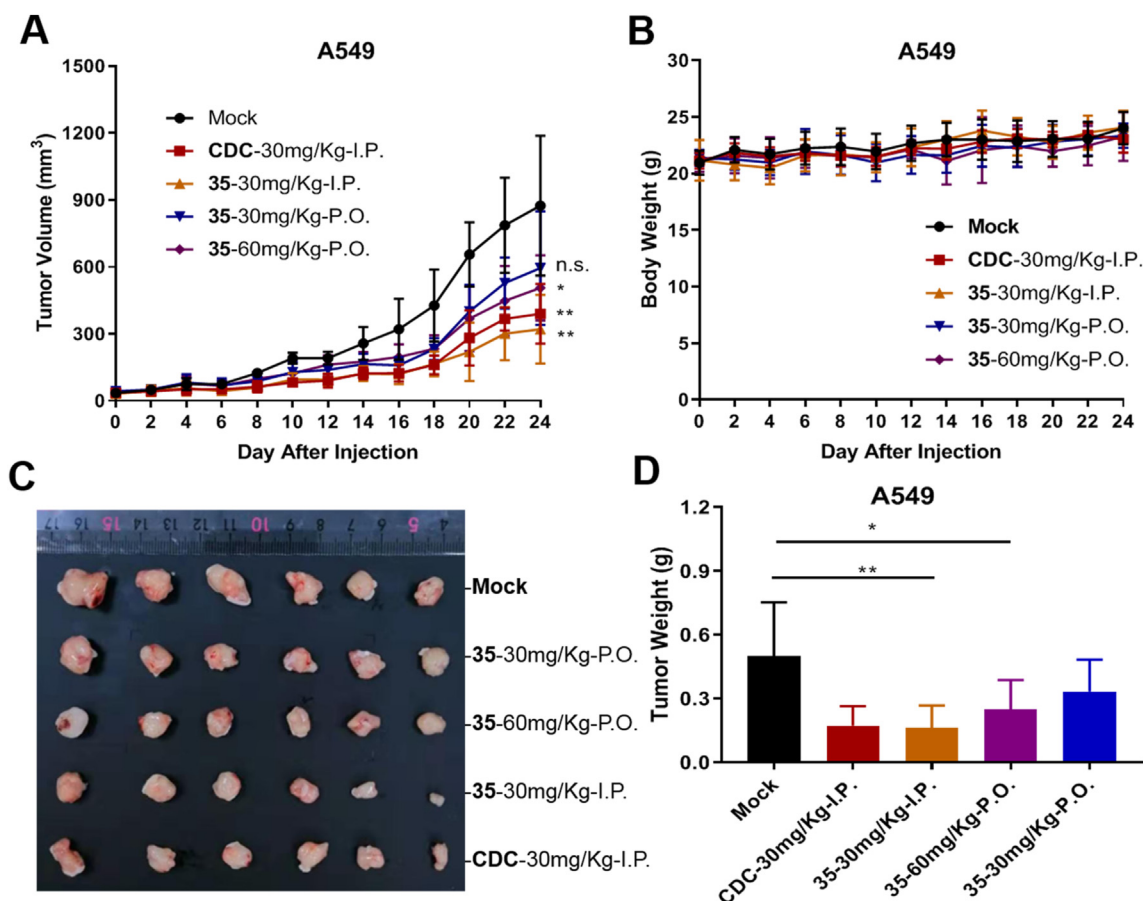


**Fig. 5.** **35** inhibited A549 xenograft growth in nude mice ( $n = 6$ ). After intraperitoneally administering vehicle (black), CDC (30 mg/kg I.P.; red), **35** (30 mg/kg I.P.; yellow), **35** (60 mg/kg P.O.; brown), **35** (30 mg/kg P.O.; blue) for three weeks, the mice were sacrificed, and the tumors were weighed. (A) Tumor volume changed during treatment; (B) Body weight changed of mice during treatment. (C) The images of tumors from mice at 24 days after initiation of treatment; (D) The tumorous weight of each group. Statistical significance was determined by the Student's *t*-test (two-tailed): \* $p < 0.05$ , \*\* $p < 0.01$ , \*\*\* $p < 0.001$ , n. s. indicates no significant difference. (For interpretation of the references to colour in this figure legend, the reader is referred to the Web version of this article.)

#### 4.2.10. 1-(((cyclohexyloxy)carbonyl)oxy)ethyl 1-([1,1'-biphenyl]-4-ylmethyl)-2-ethoxy-1H-benzo[d]imidazole-7-carboxylate (**9**)

White solid, yield 35%, mp = 178–181 °C. <sup>1</sup>H NMR (400 MHz, DMSO-*d*<sub>6</sub>)  $\delta$  7.74–7.66 (m, 2H), 7.54 (dt,  $J = 7.6, 3.8$  Hz, 1H), 7.67–7.53 (m, 1H), 7.46 (d,  $J = 7.8$  Hz, 1H), 7.45 (d,  $J = 7.7$  Hz, 1H), 7.34 (t,  $J = 7.9$  Hz, 1H), 7.12 (d,  $J = 8.2$  Hz, 2H), 6.79 (d,  $J = 8.1$  Hz, 2H), 6.76 (q,  $J = 5.3$  Hz, 2H), 5.51 (d,  $J = 6.8$  Hz, 2H), 4.63 (q,  $J = 7.0$  Hz, 2H), 4.59–4.53 (m, 1H), 4.21 (s, 3H), 1.83 (s, 2H), 1.61 (s, 2H), 1.56–1.43 (m, 9H), 1.31 (t,  $J = 12.1$  Hz, 3H). HRMS (ESI)  $m/z$  calcd C<sub>34</sub>H<sub>36</sub>N<sub>6</sub>O<sub>6</sub> [M+H]<sup>+</sup> 543.2495, found 543.2497.

#### 4.2.11. 1-(((cyclohexyloxy)carbonyl)oxy)ethyl 2-ethoxy-1-((2'-(5-oxo-2,5-dihydro-1,2,4-oxadiazol-3-yl)-[1,1'-biphenyl]-4-yl)methyl)-1H-benzo[d]imidazole-7-carboxylate (**10**)

White solid, yield 67%, mp = 182–184 °C. <sup>1</sup>H NMR (400 MHz, DMSO-*d*<sub>6</sub>)  $\delta$  7.81–7.67 (m, 2H), 7.57 (dt,  $J = 7.6, 3.8$  Hz, 1H), 7.54–7.48 (m, 1H), 7.46 (d,  $J = 7.8$  Hz, 1H), 7.39 (d,  $J = 7.7$  Hz, 1H), 7.20 (dd,  $J = 20.1, 12.2$  Hz, 1H), 7.00 (t,  $J = 12.3$  Hz, 2H), 6.88 (d,  $J = 8.1$  Hz, 2H), 6.84–6.72 (m, 1H), 5.51 (q,  $J = 16.2$  Hz, 2H), 4.70–4.48 (m, 3H), 1.81 (s, 2H), 1.61 (s, 2H), 1.47–1.35 (m, 9H), 1.23 (t,  $J = 11.1$  Hz, 3H). HRMS (ESI)  $m/z$  calcd C<sub>34</sub>H<sub>34</sub>N<sub>4</sub>O<sub>8</sub> [M+H]<sup>+</sup> 627.2455, found 627.2452.

#### 4.2.12. 1-(((cyclohexyloxy)carbonyl)oxy)ethyl 2-ethoxy-1-((2'-(1-methyl-1H-tetrazol-5-yl)-[1,1'-biphenyl]-4-yl)methyl)-1H-benzo[d]imidazole-7-carboxylate (**11**)

White solid, yield 79%, mp = 187–190 °C. <sup>1</sup>H NMR (400 MHz,

DMSO-*d*<sub>6</sub>)  $\delta$  7.76–7.68 (m, 2H), 7.57 (dt,  $J = 7.6, 3.8$  Hz, 1H), 7.54–7.49 (m, 1H), 7.46 (d,  $J = 7.8$  Hz, 1H), 7.39 (d,  $J = 7.7$  Hz, 1H), 7.22 (t,  $J = 7.9$  Hz, 1H), 7.02 (d,  $J = 8.2$  Hz, 2H), 6.88 (d,  $J = 8.1$  Hz, 2H), 6.81 (q,  $J = 5.3$  Hz, 1H), 5.51 (d,  $J = 6.8$  Hz, 2H), 4.63 (q,  $J = 7.0$  Hz, 2H), 4.59–4.53 (m, 1H), 4.21 (s, 3H), 1.81 (s, 2H), 1.61 (s, 2H), 1.45–1.33 (m, 9H), 1.23 (t,  $J = 12.1$  Hz, 3H). HRMS (ESI)  $m/z$  calcd C<sub>34</sub>H<sub>36</sub>N<sub>6</sub>O<sub>6</sub> [M+H]<sup>+</sup> 625.2775, found 625.2773.

#### 4.3. General procedure for compounds **12–46**

In round bottom flask, add candesartan (1 g, 2.27 mmol), trimethylamine (0.34 g, 3.40 mmol), 4-dimethylaminopyridine (DMAP) (0.04 g, 0.34 mmol), and trityl bromide (0.73 g, 2.27 mmol) was dissolved in dichloromethane (20 mL), and the reaction mixture was stirred at room temperature for 18 h. On completion of the reaction, 100 mL water was added to the reaction mixture at room temperature and EtOAc was extracted (3 × 50 mL), followed by brine. The organic layer was dried (MgSO<sub>4</sub>), filtered and concentrated in vacuo to give the desired crude product. Purification of the crude was done by column chromatography using dichloromethane: methanol (20:1) as solvent system, to yield the desired product **12a**. Add HOBt (103 mg, 0.76 mmol), EDCI (192 mg, 1.0 mmol), triethylamine (0.21 mL, 1.5 mmol) and **12a** (520 mg, 0.76 mmol) to round bottom flask, and dissolved in 10 mL DMF. The solution (10 mL) was stirred at room temperature for 30 min. Then, amine (0.76 mmol) was added to the reaction mixture, and the reaction was carried out at room temperature overnight. After the

reaction was completed, it was quenched with water and extracted with EtOAc (3 × 50 mL). The organic phase was collected, dried over anhydrous MgSO<sub>4</sub>, and finally the solvent was removed under reduced pressure. The crude product was used directly in the next step without further purification. The corresponding amide compound was dissolved in dichloromethane, and trifluoroacetic acid was added dropwise under ice bath, the reaction was carried out at room temperature for 3 h. After the reaction was completed, it was quenched with water and extracted with EtOAc (3 × 50 mL). The organic phase was collected, dried over anhydrous MgSO<sub>4</sub>, and finally the solvent was removed under reduced pressure to obtain the crude product. The crude product was purified by silica gel column chromatography (CH<sub>2</sub>Cl<sub>2</sub>: MeOH = 10: 1) to afford compounds **12–46**.

#### 4.3.1. 1-((2'-(1H-tetrazol-5-yl)-[1,1'-biphenyl]-4-yl)methyl)-2-ethoxy-N-phenyl-1H-benzod[imidazole-7-carboxamide (**12**)

White solid, yield 77%, mp = 182–185 °C. <sup>1</sup>H NMR (400 MHz, DMSO-*d*<sub>6</sub>) δ 7.76 (t, *J* = 5.5 Hz, 1H), 7.70 (dd, *J* = 7.5, 1.4 Hz, 1H), 7.50–7.46 (m, 1H), 7.38–7.31 (m, 2H), 7.31–7.28 (m, 1H), 7.17 (dt, *J* = 3.2, 1.6 Hz, 1H), 7.09–7.04 (m, 1H), 7.00 (d, *J* = 8.3 Hz, 2H), 6.82 (d, *J* = 8.3 Hz, 2H), 5.44 (s, 2H), 4.64 (q, *J* = 7.1 Hz, 2H), 3.18–3.15 (m, 2H), 1.52 (dd, *J* = 14.5, 7.3 Hz, 2H), 1.46 (dd, *J* = 9.5, 4.7 Hz, 3H), 0.88 (t, *J* = 7.4 Hz, 3H). <sup>13</sup>C NMR (151 MHz, DMSO-*d*<sub>6</sub>) δ 166.36, 160.01, 140.42, 140.35, 134.38, 131.86, 129.83, 129.31, 128.93, 128.55, 126.60, 126.05, 125.30, 121.20, 120.12, 119.80, 118.29, 69.17, 65.68, 44.84, 44.49, 40.36, 33.43, 28.40, 21.40, 15.10, 13.86, 13.33, 10.87. HRMS (ESI) *m/z* calcd C<sub>27</sub>H<sub>27</sub>N<sub>7</sub>O<sub>2</sub> [M+H]<sup>+</sup> 482.2304, found 482.2306.

#### 4.3.2. 1-((2'-(1H-tetrazol-5-yl)-[1,1'-biphenyl]-4-yl)methyl)-N-cyclopropyl-2-ethoxy-1H-benzod[imidazole-7-carboxamide (**13**)

White solid, yield 83%, mp = 195–198 °C. <sup>1</sup>H NMR (400 MHz, DMSO-*d*<sub>6</sub>) δ 8.40 (d, *J* = 4.5 Hz, 1H), 7.99 (d, *J* = 8.4 Hz, 1H), 7.73 (d, *J* = 8.4 Hz, 1H), 7.68–7.62 (m, 2H), 7.60–7.50 (m, 3H), 7.49–7.39 (m, 2H), 7.15–7.05 (m, 2H), 5.76 (s, 1H), 5.42 (s, 2H), 4.57 (q, *J* = 7.0 Hz, 2H), 2.80–2.70 (m, 1H), 1.38 (t, *J* = 7.1 Hz, 3H), 0.59 (tt, *J* = 10.1, 5.2 Hz, 2H), 0.38–0.31 (m, 2H). HRMS (ESI) *m/z* calcd C<sub>27</sub>H<sub>25</sub>N<sub>7</sub>O<sub>2</sub> [M+H]<sup>+</sup> 480.2148, found 480.2149.

#### 4.3.3. 1-((2'-(1H-tetrazol-5-yl)-[1,1'-biphenyl]-4-yl)methyl)-N-cyclopentyl-2-ethoxy-1H-benzod[imidazole-7-carboxamide (**14**)

White solid, yield 75%, mp = 173–175 °C. <sup>1</sup>H NMR (400 MHz, DMSO-*d*<sub>6</sub>) δ 8.37 (d, *J* = 7.3 Hz, 1H), 7.66 (dd, *J* = 16.4, 7.7 Hz, 2H), 7.60–7.50 (m, 2H), 7.45 (d, *J* = 7.7 Hz, 1H), 7.16–7.07 (m, 2H), 7.04–6.92 (m, 4H), 5.42 (s, 2H), 4.56 (q, *J* = 7.0 Hz, 2H), 4.11 (dq, *J* = 14.0, 7.0 Hz, 1H), 1.72 (dt, *J* = 12.4, 6.2 Hz, 2H), 1.56 (dd, *J* = 14.1, 7.3 Hz, 2H), 1.47 (dd, *J* = 14.3, 7.5 Hz, 2H), 1.38 (t, *J* = 7.1 Hz, 3H), 1.36–1.29 (m, 2H). <sup>13</sup>C NMR (101 MHz, DMSO-*d*<sub>6</sub>) δ 166.94, 158.15, 141.47, 141.40, 138.69, 137.08, 131.49, 131.12, 130.99, 130.03, 129.39, 128.24, 127.18, 123.94, 122.07, 121.42, 120.92, 119.36, 66.76, 51.26, 45.92, 32.37, 23.94, 14.91. HRMS (ESI) *m/z* calcd C<sub>29</sub>H<sub>29</sub>N<sub>7</sub>O<sub>2</sub> [M+H]<sup>+</sup> 508.2461, found 508.2460.

#### 4.3.4. 1-((2'-(1H-tetrazol-5-yl)-[1,1'-biphenyl]-4-yl)methyl)-N-cyclohexyl-2-ethoxy-1H-benzod[imidazole-7-carboxamide (**15**)

White solid, yield 66%, mp = 191–195 °C. <sup>1</sup>H NMR (400 MHz, DMSO-*d*<sub>6</sub>) δ 8.28 (t, *J* = 12.7 Hz, 1H), 7.65 (dd, *J* = 15.6, 7.8 Hz, 2H), 7.59–7.49 (m, 2H), 7.44 (d, *J* = 7.5 Hz, 1H), 7.12 (q, *J* = 7.2 Hz, 2H), 7.02–6.87 (m, 4H), 5.41 (d, *J* = 7.9 Hz, 2H), 4.55 (q, *J* = 7.1 Hz, 2H), 3.67–3.57 (m, 1H), 1.70–1.49 (m, 6H), 1.37 (dd, *J* = 12.7, 5.7 Hz, 3H), 1.23 (t, *J* = 14.8, 9.2 Hz, 3H), 1.11 (d, *J* = 7.6 Hz, 1H). <sup>13</sup>C NMR (151 MHz, DMSO-*d*<sub>6</sub>) δ 165.45, 157.08, 140.40, 140.34, 136.07, 130.50, 130.06, 129.89, 128.96, 128.27, 127.19, 126.11, 121.06, 120.32, 119.86, 118.29, 65.67, 47.59, 44.87, 31.37, 24.54, 24.06, 13.82. HRMS (ESI) *m/z* calcd C<sub>30</sub>H<sub>31</sub>N<sub>7</sub>O<sub>2</sub> [M+H]<sup>+</sup> 522.2617, found 522.2618.

#### 4.3.5. 1-((2'-(1H-tetrazol-5-yl)-[1,1'-biphenyl]-4-yl)methyl)-N-(3-(dimethylamino)propyl)-2-ethoxy-1H-benzod[imidazole-7-carboxamide (**16**)

Gray solid, yield 67%, mp = 198–200 °C. <sup>1</sup>H NMR (400 MHz, DMSO-*d*<sub>6</sub>) δ 8.52 (t, *J* = 5.8 Hz, 1H), 7.60–7.53 (m, 2H), 7.46–7.37 (m, 2H), 7.38–7.31 (m, 1H), 7.19–7.10 (m, 2H), 6.99 (d, *J* = 8.2 Hz, 2H), 6.78 (d, *J* = 8.2 Hz, 2H), 5.45 (s, 2H), 4.55 (q, *J* = 7.0 Hz, 2H), 3.22–3.18 (m, 2H), 2.95–2.86 (m, 2H), 2.63 (s, 6H), 1.60 (dd, *J* = 14.6, 7.1 Hz, 2H), 1.36 (t, *J* = 7.0 Hz, 3H). HRMS (ESI) *m/z* calcd C<sub>29</sub>H<sub>32</sub>N<sub>8</sub>O<sub>2</sub> [M+H]<sup>+</sup> 525.2726, found 525.2727.

#### 4.3.6. 1-((2'-(1H-tetrazol-5-yl)-[1,1'-biphenyl]-4-yl)methyl)-2-ethoxy-N-(3-methoxypropyl)-1H-benzod[imidazole-7-carboxamide (**17**)

Gray solid, yield 87%, mp = 176–180 °C. <sup>1</sup>H NMR (400 MHz, DMSO-*d*<sub>6</sub>) δ 8.35 (t, *J* = 5.6 Hz, 1H), 7.70–7.61 (m, 2H), 7.60–7.51 (m, 2H), 7.47 (d, *J* = 7.5 Hz, 1H), 7.16–7.10 (m, 2H), 7.02–6.91 (m, 4H), 5.76 (s, 1H), 5.41 (s, 2H), 4.61–4.53 (m, 2H), 3.27 (t, *J* = 6.2 Hz, 2H), 3.21–3.12 (m, 5H), 1.62–1.53 (m, 2H), 1.38 (t, *J* = 8.7, 5.4 Hz, 3H). HRMS (ESI) *m/z* calcd C<sub>28</sub>H<sub>29</sub>N<sub>7</sub>O<sub>3</sub> [M+H]<sup>+</sup> 512.2410, found 512.2411.

#### 4.3.7. 1-((2'-(1H-tetrazol-5-yl)-[1,1'-biphenyl]-4-yl)methyl)-N-(3-(cyclohexylamino)propyl)-2-ethoxy-1H-benzod[imidazole-7-carboxamide (**18**)

White solid, yield 87%, mp = 191–195 °C. <sup>1</sup>H NMR (400 MHz, DMSO-*d*<sub>6</sub>) δ 8.50 (t, *J* = 5.7 Hz, 1H), 7.61–7.49 (m, 2H), 7.46–7.33 (m, 3H), 7.21–7.11 (m, 2H), 6.97 (d, *J* = 8.2 Hz, 2H), 6.77 (d, *J* = 8.2 Hz, 2H), 5.46 (s, 2H), 4.53 (q, *J* = 7.0 Hz, 2H), 3.22–3.14 (m, 2H), 2.71 (d, *J* = 33.9 Hz, 3H), 1.87 (s, 2H), 1.70–1.46 (m, 5H), 1.36 (t, *J* = 7.0 Hz, 3H), 1.16 (dd, *J* = 19.2, 12.1 Hz, 4H), 0.94 (s, 2H). HRMS (ESI) *m/z* calcd C<sub>33</sub>H<sub>38</sub>N<sub>8</sub>O<sub>2</sub> [M+H]<sup>+</sup> 579.3196, found 579.3198.

#### 4.3.8. Ethyl 1-((2'-(1H-tetrazol-5-yl)-[1,1'-biphenyl]-4-yl)methyl)-2-ethoxy-1H-benzod[imidazole-7-carboxyl]glycinate (**19**)

White solid, yield 62%, mp = 190–192 °C. <sup>1</sup>H NMR (400 MHz, DMSO-*d*<sub>6</sub>) δ 8.73 (t, *J* = 5.9 Hz, 1H), 7.94–7.83 (m, 4H), 7.59–7.54 (m, 2H), 7.47 (ddd, *J* = 14.8, 7.7, 1.2 Hz, 2H), 7.42–7.39 (m, 1H), 7.18–7.13 (m, 1H), 7.11–7.06 (m, 1H), 5.31 (s, 2H), 4.50 (dq, *J* = 14.2, 7.1 Hz, 2H), 4.07–3.98 (m, 2H), 3.85 (t, *J* = 9.1 Hz, 2H), 1.29 (t, *J* = 7.0 Hz, 3H), 1.11 (t, *J* = 7.1 Hz, 3H). HRMS (ESI) *m/z* calcd C<sub>28</sub>H<sub>27</sub>N<sub>7</sub>O<sub>4</sub> [M+H]<sup>+</sup> 526.2203, found 526.2204.

#### 4.3.9. Methyl (1*r*,4*r*)-4-(1-((2'-(1H-tetrazol-5-yl)-[1,1'-biphenyl]-4-yl)methyl)-2-ethoxy-1H-benzod[imidazole-7-carboxamido)cyclohexane-1-carboxylate (**20**)

White solid, yield 68%, mp = 182–185 °C. <sup>1</sup>H NMR (400 MHz, DMSO-*d*<sub>6</sub>) δ 8.33 (d, *J* = 7.7 Hz, 1H), 7.96 (s, 1H), 7.72–7.61 (m, 2H), 7.60–7.51 (m, 2H), 7.45 (d, *J* = 7.7 Hz, 1H), 7.18–7.08 (m, 2H), 7.05–6.94 (m, 4H), 5.47 (d, *J* = 32.9 Hz, 2H), 4.58 (dq, *J* = 14.2, 7.1 Hz, 2H), 3.48–3.41 (m, 1H), 3.18 (s, 3H), 2.29–2.14 (m, 1H), 1.90 (dd, *J* = 14.2, 3.6 Hz, 2H), 1.70 (dd, *J* = 12.9, 3.9 Hz, 2H), 1.44–1.35 (m, 4H), 1.26–1.04 (t, 3H). HRMS (ESI) *m/z* calcd C<sub>32</sub>H<sub>33</sub>N<sub>7</sub>O<sub>4</sub> [M+H]<sup>+</sup> 580.2672, found 580.2673.

#### 4.3.10. 1-((2'-(1H-tetrazol-5-yl)-[1,1'-biphenyl]-4-yl)methyl)-2-ethoxy-N-propyl-1H-benzod[imidazole-7-carboxamide (**21**)

White solid, yield 72%, mp = 202–205 °C. <sup>1</sup>H NMR (400 MHz, DMSO-*d*<sub>6</sub>) δ 10.35 (s, 1H), 7.68–7.58 (m, 5H), 7.58–7.52 (m, 1H), 7.32 (t, *J* = 7.7 Hz, 3H), 7.27 (d, *J* = 7.2 Hz, 1H), 7.20 (t, *J* = 7.7 Hz, 1H), 7.10 (t, *J* = 7.4 Hz, 1H), 7.01 (d, *J* = 8.5 Hz, 1H), 6.90 (d, *J* = 8.1 Hz, 2H), 6.80 (d, *J* = 8.1 Hz, 2H), 5.35 (s, 2H), 4.68–4.54 (q, 2H), 1.40 (t, *J* = 13.6, 6.6 Hz, 3H). <sup>13</sup>C NMR (151 MHz, DMSO-*d*<sub>6</sub>) δ 166.10, 158.28, 141.63, 141.40, 139.57, 136.59, 131.46, 131.03, 129.90, 129.31, 129.04, 128.25, 127.36, 124.19, 121.88, 121.29, 121.13, 120.38, 119.86, 66.92, 46.03,

14.92. HRMS (ESI)  $m/z$  calcd  $C_{30}H_{25}N_7O_2$   $[M+H]^+$  516.2148, found 516.2147.

4.3.11. 1-((2'-(1H-tetrazol-5-yl)-[1,1'-biphenyl]-4-yl)methyl)-2-ethoxy-N-(4-fluorophenyl)-1H-benzo[d]imidazole-7-carboxamide (22)

White solid, yield 82%, mp = 187–190 °C.  $^1H$  NMR (400 MHz, DMSO- $d_6$ )  $\delta$  10.39 (s, 1H), 7.71–7.59 (m, 5H), 7.54 (dd,  $J$  = 10.7, 4.3 Hz, 1H), 7.32 (d,  $J$  = 7.7 Hz, 1H), 7.26 (d,  $J$  = 6.6 Hz, 1H), 7.22–7.11 (m, 3H), 6.87 (d,  $J$  = 8.2 Hz, 2H), 6.81 (d,  $J$  = 8.2 Hz, 2H), 5.76 (s, 1H), 5.34 (s, 2H), 4.60 (q,  $J$  = 7.1 Hz, 2H), 1.41 (t,  $J$  = 7.1 Hz, 3H).  $^{13}C$  NMR (151 MHz, DMSO- $d_6$ )  $\delta$  165.39, 158.97, 157.72, 157.38, 141.06, 140.80, 138.19, 135.97, 135.35, 130.81, 130.46, 130.41, 129.33, 128.73, 127.66, 126.65, 121.58, 121.52, 121.13, 120.67, 120.57, 119.35, 115.11, 114.97, 66.36, 45.45, 14.34. HRMS (ESI)  $m/z$  calcd  $C_{30}H_{24}FN_7O_2$   $[M+H]^+$  534.2054, found 534.2053.

4.3.12. 1-((2'-(1H-tetrazol-5-yl)-[1,1'-biphenyl]-4-yl)methyl)-2-ethoxy-N-(4-methoxyphenyl)-1H-benzo[d]imidazole-7-carboxamide (23)

White solid, yield 59%, mp = 185–188 °C.  $^1H$  NMR (400 MHz, DMSO- $d_6$ )  $\delta$  10.23 (s, 1H), 7.68–7.50 (m, 6H), 7.35 (d,  $J$  = 7.7 Hz, 1H), 7.25 (d,  $J$  = 6.6 Hz, 1H), 7.18 (t,  $J$  = 7.7 Hz, 1H), 6.90 (dd,  $J$  = 8.5, 6.7 Hz, 4H), 6.83 (d,  $J$  = 8.2 Hz, 2H), 5.35 (s, 2H), 4.59 (q,  $J$  = 7.0 Hz, 2H), 3.74 (s, 3H), 1.40 (t,  $J$  = 7.0 Hz, 3H).  $^{13}C$  NMR (151 MHz, DMSO- $d_6$ )  $\delta$  165.13, 157.68, 155.46, 141.02, 140.78, 138.27, 136.03, 132.09, 130.72, 130.47, 130.45, 129.35, 128.75, 127.63, 126.80, 121.40, 120.68, 120.54, 119.15, 113.61, 66.31, 55.07, 53.34, 14.34. HRMS (ESI)  $m/z$  calcd  $C_{31}H_{27}N_7O_3$   $[M+H]^+$  546.2254, found 546.2255.

4.3.13. 1-((2'-(1H-tetrazol-5-yl)-[1,1'-biphenyl]-4-yl)methyl)-2-ethoxy-N-(4-sulfamoylphenyl)-1H-benzo[d]imidazole-7-carboxamide (24)

Brown solid, yield 35%, mp = 201–204 °C.  $^1H$  NMR (400 MHz, DMSO- $d_6$ )  $\delta$  10.39 (s, 1H), 7.69–7.56 (m, 5H), 7.54 (dd,  $J$  = 10.7, 4.3 Hz, 1H), 7.32 (d,  $J$  = 7.7 Hz, 1H), 7.26 (d,  $J$  = 6.6 Hz, 1H), 7.31–7.15 (m, 3H), 6.98 (s, 2H), 6.87 (d,  $J$  = 8.2 Hz, 2H), 6.81 (d,  $J$  = 8.2 Hz, 2H), 5.68 (s, 1H), 5.24 (s, 2H), 4.60 (q,  $J$  = 7.1 Hz, 2H), 1.41 (t,  $J$  = 7.1 Hz, 3H). HRMS (ESI)  $m/z$  calcd  $C_{30}H_{26}N_8O_4S$   $[M+H]^+$  595.1876, found 595.1831.

4.3.14. 1-((2'-(1H-tetrazol-5-yl)-[1,1'-biphenyl]-4-yl)methyl)-2-ethoxy-N-(pyridin-4-yl)-1H-benzo[d]imidazole-7-carboxamide (25)

White solid, yield 90%, mp = 197–199 °C.  $^1H$  NMR (400 MHz, DMSO- $d_6$ )  $\delta$  11.12 (s, 1H), 8.62–8.51 (m, 2H), 7.87 (d,  $J$  = 6.5 Hz, 2H), 7.69 (dd,  $J$  = 7.8, 1.0 Hz, 1H), 7.66–7.58 (m, 2H), 7.57–7.49 (m, 1H), 7.31 (d,  $J$  = 6.6 Hz, 1H), 7.25 (t,  $J$  = 7.7 Hz, 2H), 6.84–6.74 (m, 4H), 5.76 (s, 1H), 5.33 (s, 2H), 4.63 (q,  $J$  = 7.1 Hz, 2H), 1.42 (t,  $J$  = 7.1 Hz, 3H).  $^{13}C$  NMR (151 MHz, DMSO- $d_6$ )  $\delta$  166.15, 157.44, 154.33, 150.55, 149.09, 145.25, 140.74, 140.25, 137.67, 135.09, 130.40, 129.95, 129.87, 128.84, 128.31, 128.27, 127.24, 125.84, 122.62, 120.29, 120.20, 120.16, 119.84, 119.33, 113.69, 66.11, 45.19, 13.83. HRMS (ESI)  $m/z$  calcd  $C_{29}H_{24}N_8O_2$   $[M+H]^+$  517.2100, found 517.2101.

4.3.15. 1-((2'-(1H-tetrazol-5-yl)-[1,1'-biphenyl]-4-yl)methyl)-2-ethoxy-N-(furan-2-ylmethyl)-1H-benzo[d]imidazole-7-carboxamide (26)

White solid, yield 91%, mp = 202–204 °C.  $^1H$  NMR (400 MHz, DMSO- $d_6$ )  $\delta$  8.92 (t,  $J$  = 5.8 Hz, 1H), 7.69–7.61 (m, 2H), 7.60–7.50 (m, 3H), 7.46 (d,  $J$  = 7.6 Hz, 1H), 7.14 (dt,  $J$  = 15.1, 6.9 Hz, 2H), 7.00–6.89 (m, 4H), 6.34 (dd,  $J$  = 3.1, 1.9 Hz, 1H), 6.21 (d,  $J$  = 3.0 Hz, 1H), 5.38 (s, 2H), 4.57 (q,  $J$  = 7.1 Hz, 2H), 4.36 (d,  $J$  = 5.7 Hz, 2H), 1.39 (t,  $J$  = 7.0 Hz, 3H).  $^{13}C$  NMR (151 MHz, DMSO- $d_6$ )  $\delta$  166.25, 157.21, 151.45, 141.42, 140.49, 140.39, 137.61, 135.85, 130.44, 130.02, 129.08, 128.32, 127.17,

126.36, 120.31, 120.21, 119.93, 118.71, 109.86, 106.30, 65.72, 44.91, 35.38, 13.82. HRMS (ESI)  $m/z$  calcd  $C_{29}H_{25}N_7O_3$   $[M+H]^+$  520.2097, found 520.2098.

4.3.16. 1-((2'-(1H-tetrazol-5-yl)-[1,1'-biphenyl]-4-yl)methyl)-N-(benzo[d][1,3]dioxol-5-yl)-2-ethoxy-1H-benzo[d]imidazole-7-carboxamide (27)

White solid, yield 78%, mp = 192–195 °C.  $^1H$  NMR (400 MHz, DMSO- $d_6$ )  $\delta$  10.25 (s, 1H), 7.59 (dtd,  $J$  = 21.9, 14.5, 7.4 Hz, 4H), 7.35 (d,  $J$  = 7.7 Hz, 1H), 7.28 (d,  $J$  = 1.5 Hz, 1H), 7.25–7.15 (m, 2H), 7.05 (d,  $J$  = 8.3 Hz, 1H), 6.95–6.78 (m, 5H), 5.99 (s, 2H), 5.34 (s, 2H), 4.60 (q,  $J$  = 7.0 Hz, 2H), 1.40 (t,  $J$  = 7.0 Hz, 3H).  $^{13}C$  NMR (151 MHz, DMSO- $d_6$ )  $\delta$  164.67, 157.20, 146.31, 142.64, 140.53, 140.34, 137.66, 135.54, 132.84, 130.36, 129.97, 129.94, 128.82, 128.24, 127.17, 126.21, 120.81, 120.14, 120.06, 118.73, 112.26, 107.29, 101.35, 100.39, 65.84, 44.94, 13.83. HRMS (ESI)  $m/z$  calcd  $C_{31}H_{25}N_7O_4$   $[M+H]^+$  560.2046, found 560.2045.

4.3.17. 1-((2'-(1H-tetrazol-5-yl)-[1,1'-biphenyl]-4-yl)methyl)-N-benzyl-2-ethoxy-1H-benzo[d]imidazole-7-carboxamide (28)

White solid, yield 63%, mp = 181–184 °C.  $^1H$  NMR (400 MHz, DMSO- $d_6$ )  $\delta$  8.91 (t,  $J$  = 6.0 Hz, 1H), 7.57–7.51 (m, 2H), 7.49–7.44 (m, 2H), 7.38 (dt,  $J$  = 4.9, 3.2 Hz, 4H), 7.28 (dd,  $J$  = 7.3, 5.8, 4.1 Hz, 4H), 7.20 (dd,  $J$  = 5.2, 4.2 Hz, 1H), 7.12 (t,  $J$  = 7.7 Hz, 1H), 6.97 (t,  $J$  = 7.7 Hz, 2H), 6.79 (d,  $J$  = 8.2 Hz, 2H), 5.37 (s, 2H), 4.60 (q,  $J$  = 7.0 Hz, 2H), 4.00 (s, 2H), 1.41 (t,  $J$  = 7.0 Hz, 3H).  $^{13}C$  NMR (151 MHz, DMSO- $d_6$ )  $\delta$  166.39, 159.22, 157.25, 140.49, 139.87, 139.50, 138.78, 134.56, 133.53, 130.26, 129.85, 129.48, 129.02, 128.54, 128.26, 128.00, 127.83, 127.63, 127.30, 126.71, 126.29, 126.08, 125.49, 120.77, 120.17, 119.91, 118.56, 65.72, 41.93, 41.65, 13.85. HRMS (ESI)  $m/z$  calcd  $C_{31}H_{27}N_7O_2$   $[M+H]^+$  530.2304, found 530.2303.

4.3.18. 1-((2'-(1H-tetrazol-5-yl)-[1,1'-biphenyl]-4-yl)methyl)-2-ethoxy-N-(4-fluorobenzyl)-1H-benzo[d]imidazole-7-carboxamide (29)

White solid, yield 77%, mp = 178–190 °C.  $^1H$  NMR (400 MHz, DMSO- $d_6$ )  $\delta$  8.91 (t,  $J$  = 6.0 Hz, 1H), 7.60 (dd,  $J$  = 7.5, 1.1 Hz, 1H), 7.55–7.52 (m, 1H), 7.45 (td,  $J$  = 7.5, 1.2 Hz, 1H), 7.40–7.22 (m, 4H), 7.21–7.05 (m, 4H), 7.00–6.92 (m, 2H), 6.83 (d,  $J$  = 8.2 Hz, 2H), 5.38 (s, 2H), 4.58 (q,  $J$  = 7.0 Hz, 2H), 4.32 (d,  $J$  = 5.9 Hz, 2H), 1.39 (t,  $J$  = 7.0 Hz, 3H).  $^{13}C$  NMR (151 MHz, DMSO- $d_6$ )  $\delta$  166.35, 161.31, 159.70, 157.24, 155.85, 140.50, 140.12, 138.27, 135.51, 134.86, 130.71, 130.66, 129.98, 129.83, 129.49, 129.07, 128.72, 128.67, 128.38, 126.92, 125.86, 125.01, 120.52, 120.17, 119.95, 118.65, 114.94, 114.80, 114.42, 114.28, 65.73, 44.91, 41.26, 13.82. HRMS (ESI)  $m/z$  calcd  $C_{31}H_{26}FN_7O_2$   $[M+H]^+$  548.2210, found 548.2211.

4.3.19. 1-((2'-(1H-tetrazol-5-yl)-[1,1'-biphenyl]-4-yl)methyl)-N-benzhydryl-2-ethoxy-1H-benzo[d]imidazole-7-carboxamide (30)

White solid, yield 76%, mp = 168–170 °C.  $^1H$  NMR (400 MHz, DMSO- $d_6$ )  $\delta$  9.57 (d,  $J$  = 9.0 Hz, 1H), 7.67–7.60 (m, 2H), 7.54 (dd,  $J$  = 12.7, 7.8 Hz, 2H), 7.49–7.42 (m, 1H), 7.38 (d,  $J$  = 7.3 Hz, 4H), 7.28 (t,  $J$  = 7.2 Hz, 5H), 7.24–7.12 (m, 3H), 6.83 (d,  $J$  = 8.0 Hz, 2H), 6.67 (d,  $J$  = 8.1 Hz, 2H), 6.44 (d,  $J$  = 9.1 Hz, 1H), 5.34 (s, 2H), 4.58 (q,  $J$  = 7.0 Hz, 2H), 3.17 (s, 1H), 1.39 (t,  $J$  = 7.0 Hz, 3H).  $^{13}C$  NMR (151 MHz, DMSO- $d_6$ )  $\delta$  165.62, 157.19, 141.74, 140.50, 140.05, 137.93, 135.46, 130.04, 129.91, 129.84, 129.22, 128.33, 128.30, 127.85, 127.79, 127.02, 126.81, 126.59, 126.36, 120.99, 119.95, 119.81, 118.86, 65.73, 55.73, 44.76, 13.83. HRMS (ESI)  $m/z$  calcd  $C_{37}H_{31}N_7O_2$   $[M+H]^+$  606.2617, found 606.2618.

4.3.20. 1-((2'-(1H-tetrazol-5-yl)-[1,1'-biphenyl]-4-yl)methyl)-N-(benzo[d][1,3]dioxol-5-ylmethyl)-2-ethoxy-1H-benzo[d]imidazole-7-carboxamide (31)

White solid, yield 78%, mp = 193–195 °C.  $^1H$  NMR (400 MHz,

DMSO- $d_6$ )  $\delta$  8.89 (t,  $J$  = 5.9 Hz, 1H), 7.70–7.62 (m, 2H), 7.60–7.52 (m, 2H), 7.45 (d,  $J$  = 7.6 Hz, 1H), 7.22–7.10 (m, 2H), 6.97–6.93 (m, 2H), 6.88 (dd,  $J$  = 9.3, 4.8 Hz, 3H), 6.78 (dt,  $J$  = 7.9, 4.7 Hz, 2H), 5.94 (d,  $J$  = 4.0 Hz, 2H), 5.39 (s, 2H), 4.58 (q,  $J$  = 7.1 Hz, 2H), 4.26 (d,  $J$  = 6.1 Hz, 2H), 1.39 (t,  $J$  = 7.1 Hz, 3H).  $^{13}\text{C}$  NMR (151 MHz, DMSO- $d_6$ )  $\delta$  166.71, 157.72, 147.07, 145.92, 140.99, 140.92, 138.14, 136.35, 133.00, 130.89, 130.54, 130.48, 129.57, 128.80, 127.66, 126.67, 121.01, 120.71, 120.54, 120.46, 119.13, 108.02, 107.88, 100.67, 66.23, 45.41, 42.28, 13.83. HRMS (ESI)  $m/z$  calcd  $\text{C}_{32}\text{H}_{27}\text{N}_7\text{O}_4$   $[\text{M}+\text{H}]^+$  574.2203, found 574.2204.

4.3.21. 1-((2'-(1H-tetrazol-5-yl)-[1,1'-biphenyl]-4-yl)methyl)-2-ethoxy-N-phenethyl-1H-benzo[d]imidazole-7-carboxamide (**32**)

White solid, yield 92%, mp = 192–195 °C.  $^1\text{H}$  NMR (400 MHz, DMSO- $d_6$ )  $\delta$  8.41 (t,  $J$  = 5.5 Hz, 1H), 7.63 (t,  $J$  = 6.4 Hz, 2H), 7.54 (t,  $J$  = 7.5 Hz, 2H), 7.42 (d,  $J$  = 7.5 Hz, 1H), 7.31–7.23 (m, 2H), 7.23–7.15 (m, 3H), 7.09 (dt,  $J$  = 7.5, 7.1 Hz, 2H), 6.96 (q,  $J$  = 8.3 Hz, 4H), 5.76 (s, 1H), 5.39 (s, 2H), 4.56 (q,  $J$  = 7.1 Hz, 2H), 3.39–3.34 (m, 2H), 2.67 (t,  $J$  = 7.4 Hz, 2H), 1.37 (t,  $J$  = 7.0 Hz, 3H).  $^{13}\text{C}$  NMR (151 MHz, DMSO- $d_6$ )  $\delta$  166.28, 157.19, 140.45, 140.42, 138.80, 136.05, 130.42, 130.01, 129.98, 129.01, 128.31, 128.03, 127.71, 127.18, 126.03, 125.49, 120.85, 120.03, 119.92, 118.47, 65.71, 54.31, 40.08, 34.14, 13.82. HRMS (ESI)  $m/z$  calcd  $\text{C}_{32}\text{H}_{29}\text{N}_7\text{O}_2$   $[\text{M}+\text{H}]^+$  544.2461, found 544.2462.

4.3.22. 1-((2'-(1H-tetrazol-5-yl)-[1,1'-biphenyl]-4-yl)methyl)-N-(4-bromophenethyl)-2-ethoxy-1H-benzo[d]imidazole-7-carboxamide (**33**)

White solid, yield 89%, mp = 205–207 °C.  $^1\text{H}$  NMR (400 MHz, DMSO- $d_6$ )  $\delta$  8.42 (t,  $J$  = 5.6 Hz, 1H), 7.67–7.59 (m, 2H), 7.54 (td,  $J$  = 7.7, 1.2 Hz, 2H), 7.50–7.38 (m, 4H), 7.15 (s, 1H), 7.12 (dd,  $J$  = 10.6, 4.8 Hz, 2H), 7.05 (dd,  $J$  = 7.6, 1.1 Hz, 1H), 6.98 (d,  $J$  = 8.3 Hz, 2H), 6.92 (d,  $J$  = 8.3 Hz, 2H), 5.37 (s, 2H), 4.56 (q,  $J$  = 7.0 Hz, 2H), 2.64 (t,  $J$  = 7.2 Hz, 2H), 1.37 (t,  $J$  = 7.1 Hz, 3H).  $^{13}\text{C}$  NMR (151 MHz, DMSO- $d_6$ )  $\delta$  166.79, 157.70, 140.89, 138.80, 138.11, 136.51, 131.01, 130.87, 130.51, 130.47, 129.50, 128.81, 127.73, 127.66, 127.23, 126.45, 124.41, 121.26, 120.50, 120.44, 119.03, 119.00, 109.54, 66.21, 45.43, 40.22, 33.97, 14.31. HRMS (ESI)  $m/z$  calcd  $\text{C}_{32}\text{H}_{28}\text{BrN}_7\text{O}_2$   $[\text{M}+\text{H}]^+$  622.1566, found 622.1565.

4.3.23. 1-((2'-(1H-tetrazol-5-yl)-[1,1'-biphenyl]-4-yl)methyl)-2-ethoxy-N-(4-nitrophenethyl)-1H-benzo[d]imidazole-7-carboxamide (**34**)

White solid, yield 56%, mp = 184–185 °C.  $^1\text{H}$  NMR (400 MHz, DMSO- $d_6$ )  $\delta$  8.44 (t,  $J$  = 5.4 Hz, 1H), 8.13 (d,  $J$  = 8.6 Hz, 2H), 7.62 (t,  $J$  = 5.5 Hz, 2H), 7.54 (t,  $J$  = 7.2 Hz, 2H), 7.47 (d,  $J$  = 8.6 Hz, 2H), 7.42 (d,  $J$  = 7.4 Hz, 1H), 7.12 (t,  $J$  = 7.7 Hz, 1H), 7.05 (d,  $J$  = 7.0 Hz, 1H), 6.98 (d,  $J$  = 8.2 Hz, 2H), 6.92 (d,  $J$  = 8.2 Hz, 2H), 5.75 (s, 1H), 5.37 (s, 2H), 4.56 (q,  $J$  = 7.0 Hz, 2H), 3.39 (dt,  $J$  = 16.2, 8.1 Hz, 2H), 2.82 (t,  $J$  = 7.0 Hz, 2H), 1.37 (t,  $J$  = 7.0 Hz, 3H).  $^{13}\text{C}$  NMR (151 MHz, DMSO- $d_6$ )  $\delta$  166.87, 157.73, 147.82, 145.98, 140.97, 140.89, 138.08, 136.53, 130.91, 130.52, 130.47, 129.94, 129.52, 128.83, 127.69, 126.43, 123.28, 121.16, 120.52, 120.46, 119.07, 66.23, 54.82, 45.46, 34.49, 14.32. HRMS (ESI)  $m/z$  calcd  $\text{C}_{32}\text{H}_{28}\text{N}_8\text{O}_4$   $[\text{M}+\text{H}]^+$  589.2312, found 589.2313.

4.3.24. 1-((2'-(1H-tetrazol-5-yl)-[1,1'-biphenyl]-4-yl)methyl)-N-(2,4-dichlorophenethyl)-2-ethoxy-1H-benzo[d]imidazole-7-carboxamide (**35**)

White solid, yield 88%, mp = 172–175 °C.  $^1\text{H}$  NMR (400 MHz, DMSO- $d_6$ )  $\delta$  8.43 (t,  $J$  = 5.6 Hz, 1H), 7.62 (t,  $J$  = 6.3 Hz, 2H), 7.58–7.50 (m, 3H), 7.42 (d,  $J$  = 7.3 Hz, 1H), 7.32 (dt,  $J$  = 14.8, 5.2 Hz, 2H), 7.10 (dt,  $J$  = 7.6, 7.1 Hz, 2H), 6.98 (d,  $J$  = 8.2 Hz, 2H), 6.92 (d,  $J$  = 8.2 Hz, 2H), 5.39 (s, 2H), 4.57 (q,  $J$  = 7.0 Hz, 2H), 3.40–3.35 (m, 2H), 2.80 (t,  $J$  = 7.0 Hz, 2H), 1.38 (t,  $J$  = 7.0 Hz, 3H).  $^{13}\text{C}$  NMR (151 MHz, DMSO- $d_6$ )  $\delta$  167.40, 158.28, 141.55, 138.71, 137.07, 136.45, 134.56, 132.84, 132.19, 131.39, 131.08, 131.03, 130.08, 129.41, 129.11, 128.23, 127.80,

127.76, 127.04, 121.77, 121.10, 121.01, 119.63, 66.81, 46.03, 38.97, 32.53, 14.89. HRMS (ESI)  $m/z$  calcd  $\text{C}_{32}\text{H}_{27}\text{Cl}_2\text{N}_7\text{O}_2$   $[\text{M}+\text{H}]^+$  612.1682, found 612.1680.

4.3.25. 1-((2'-(1H-tetrazol-5-yl)-[1,1'-biphenyl]-4-yl)methyl)-N-(benzyloxy)-2-ethoxy-1H-benzo[d]imidazole-7-carboxamide (**36**)

White solid, yield 87%, mp = 178–181 °C.  $^1\text{H}$  NMR (400 MHz, DMSO- $d_6$ )  $\delta$  11.66 (s, 1H), 7.59 (dd,  $J$  = 18.3, 15.4, 7.5 Hz, 4H), 7.43–7.31 (m, 6H), 7.12 (dt,  $J$  = 7.6, 7.0 Hz, 2H), 6.98 (s, 4H), 5.42 (s, 2H), 4.66 (s, 2H), 4.56 (q,  $J$  = 7.0 Hz, 2H), 1.36 (t,  $J$  = 7.1 Hz, 3H).  $^{13}\text{C}$  NMR (151 MHz, DMSO- $d_6$ )  $\delta$  163.46, 157.22, 140.51, 140.31, 135.94, 135.11, 130.41, 130.01, 129.97, 129.49, 128.40, 128.20, 127.70, 127.18, 125.91, 120.54, 119.99, 119.25, 117.23, 76.22, 65.82, 45.04, 13.78. HRMS (ESI)  $m/z$  calcd  $\text{C}_{31}\text{H}_{27}\text{N}_7\text{O}_3$   $[\text{M}+\text{H}]^+$  546.2254, found 546.2253.

4.3.26. 1-((2'-(1H-tetrazol-5-yl)-[1,1'-biphenyl]-4-yl)methyl)-2-ethoxy-N-(4-phenylbutyl)-1H-benzo[d]imidazole-7-carboxamide (**37**)

White solid, yield 53%, mp = 186–190 °C.  $^1\text{H}$  NMR (400 MHz, DMSO- $d_6$ )  $\delta$  8.37 (t,  $J$  = 5.6 Hz, 1H), 7.66–7.56 (m, 2H), 7.55–7.48 (m, 2H), 7.39 (d,  $J$  = 6.9 Hz, 1H), 7.30–7.18 (m, 3H), 7.12 (dt,  $J$  = 7.5, 6.2 Hz, 5H), 6.96 (d,  $J$  = 8.2 Hz, 2H), 6.91 (d,  $J$  = 8.2 Hz, 2H), 5.76 (s, 1H), 5.39 (s, 2H), 4.57 (q,  $J$  = 7.0 Hz, 2H), 3.19–3.06 (m, 2H), 2.56 (dd,  $J$  = 18.3, 7.5 Hz, 2H), 1.38 (t,  $J$  = 7.0 Hz, 4H), 1.25 (t,  $J$  = 7.4 Hz, 3H).  $^{13}\text{C}$  NMR (151 MHz, DMSO- $d_6$ )  $\delta$  166.31, 157.18, 155.62, 141.52, 140.43, 140.18, 138.16, 135.66, 129.99, 129.85, 129.65, 128.97, 128.35, 127.70, 127.66, 127.59, 126.95, 125.95, 125.00, 121.00, 120.11, 119.91, 118.38, 65.70, 52.78, 38.31, 34.14, 27.84, 27.79, 13.83. HRMS (ESI)  $m/z$  calcd  $\text{C}_{34}\text{H}_{33}\text{N}_7\text{O}_2$   $[\text{M}+\text{H}]^+$  572.2774, found 572.2775.

4.3.27. 1-((2'-(1H-tetrazol-5-yl)-[1,1'-biphenyl]-4-yl)methyl)-N-(2,6-dichlorophenethyl)-2-ethoxy-1H-benzo[d]imidazole-7-carboxamide (**38**)

White solid, yield 77%, mp = 188–190 °C.  $^1\text{H}$  NMR (400 MHz, DMSO- $d_6$ )  $\delta$  8.52 (t,  $J$  = 5.7 Hz, 1H), 7.62 (t,  $J$  = 7.1 Hz, 2H), 7.57–7.50 (m, 2H), 7.43 (dd,  $J$  = 15.9, 7.8 Hz, 3H), 7.31–7.24 (m, 1H), 7.18–7.09 (m, 2H), 6.96 (q,  $J$  = 8.3 Hz, 4H), 5.42 (s, 2H), 4.57 (q,  $J$  = 7.0 Hz, 2H), 3.38–3.33 (m, 2H), 3.04–2.95 (m, 2H), 1.38 (t,  $J$  = 7.0 Hz, 3H).  $^{13}\text{C}$  NMR (151 MHz, DMSO- $d_6$ )  $\delta$  166.25, 157.19, 140.48, 140.41, 137.61, 136.04, 134.31, 134.09, 130.33, 129.99, 129.95, 129.03, 128.49, 128.32, 127.90, 127.89, 127.16, 126.03, 120.75, 120.12, 119.91, 118.56, 65.73, 44.98, 36.69, 30.15, 13.83, 13.82. HRMS (ESI)  $m/z$  calcd  $\text{C}_{32}\text{H}_{27}\text{Cl}_2\text{N}_7\text{O}_2$   $[\text{M}+\text{H}]^+$  612.1682, found 612.1683.

4.3.28. 1-((2'-(1H-tetrazol-5-yl)-[1,1'-biphenyl]-4-yl)methyl)-N-(2,5-dichlorophenethyl)-2-ethoxy-1H-benzo[d]imidazole-7-carboxamide (**39**)

White solid, yield 89%, mp = 203–205 °C.  $^1\text{H}$  NMR (400 MHz, DMSO- $d_6$ )  $\delta$  8.43 (t,  $J$  = 5.5 Hz, 1H), 7.65–7.57 (m, 2H), 7.52 (t,  $J$  = 8.0 Hz, 2H), 7.47–7.36 (m, 3H), 7.31 (dd,  $J$  = 8.5, 2.6 Hz, 1H), 7.11 (t,  $J$  = 7.7 Hz, 1H), 7.08–7.02 (m, 1H), 6.97 (d,  $J$  = 8.2 Hz, 2H), 6.91 (d,  $J$  = 8.2 Hz, 2H), 5.37 (s, 2H), 4.57 (q,  $J$  = 7.0 Hz, 2H), 3.38 (dd,  $J$  = 12.8, 6.8 Hz, 2H), 2.83 (t,  $J$  = 6.9 Hz, 2H), 1.38 (t,  $J$  = 7.1 Hz, 3H).  $^{13}\text{C}$  NMR (151 MHz, DMSO- $d_6$ )  $\delta$  166.86, 157.72, 155.56, 140.98, 140.80, 138.94, 138.41, 136.30, 131.82, 131.49, 130.70, 130.67, 130.48, 130.41, 129.48, 128.85, 127.90, 127.56, 126.46, 124.25, 121.24, 120.47, 120.40, 119.04, 66.24, 45.45, 38.23, 32.28, 14.33. HRMS (ESI)  $m/z$  calcd  $\text{C}_{32}\text{H}_{27}\text{Cl}_2\text{N}_7\text{O}_2$   $[\text{M}+\text{H}]^+$  612.1682, found 612.1684.

4.3.29. 1-((2'-(1H-tetrazol-5-yl)-[1,1'-biphenyl]-4-yl)methyl)-2-ethoxy-N-(3-methoxyphenethyl)-1H-benzo[d]imidazole-7-carboxamide (**40**)

White solid, yield 66%, mp = 185–188 °C.  $^1\text{H}$  NMR (400 MHz, DMSO- $d_6$ )  $\delta$  8.40 (t,  $J$  = 5.5 Hz, 1H), 7.61 (dd,  $J$  = 11.8, 4.5 Hz, 2H),

7.58–7.49 (m, 2H), 7.42 (d,  $J = 7.7$  Hz, 1H), 7.22–7.15 (m, 1H), 7.15–7.04 (m, 2H), 6.98 (d,  $J = 8.3$  Hz, 2H), 6.93 (d,  $J = 8.3$  Hz, 2H), 6.76 (d,  $J = 6.6$  Hz, 3H), 5.38 (s, 2H), 4.57 (q,  $J = 7.0$  Hz, 2H), 3.71 (s, 3H), 3.34 (d,  $J = 4.9$  Hz, 2H), 2.64 (t,  $J = 7.4$  Hz, 2H), 1.38 (t,  $J = 7.1$  Hz, 3H).  $^{13}\text{C}$  NMR (151 MHz, DMSO- $d_6$ )  $\delta$  166.27, 158.66, 157.19, 140.45, 140.39, 137.68, 135.96, 130.25, 129.99, 129.95, 128.99, 128.71, 128.31, 127.13, 125.99, 120.88, 120.27, 120.01, 119.91, 118.46, 113.51, 111.09, 65.71, 54.25, 44.92, 39.96, 34.15, 13.82. HRMS (ESI)  $m/z$  calcd  $\text{C}_{33}\text{H}_{31}\text{N}_7\text{O}_3$   $[\text{M}+\text{H}]^+$  574.2567, found 574.2568.

4.3.30. 1-((2'-(1H-tetrazol-5-yl)-[1,1'-biphenyl]-4-yl)methyl)-2-ethoxy-N-(4-methylphenethyl)-1H-benzo[d]imidazole-7-carboxamide (**41**)

White solid, yield 79%, mp = 192–195 °C.  $^1\text{H}$  NMR (400 MHz, DMSO- $d_6$ )  $\delta$  8.40 (t,  $J = 5.5$  Hz, 1H), 7.61 (dd,  $J = 11.9, 4.4$  Hz, 2H), 7.53 (dd,  $J = 7.5, 4.3, 1.6$  Hz, 2H), 7.41 (d,  $J = 7.8$  Hz, 1H), 7.16–7.09 (m, 1H), 7.09–7.05 (m, 5H), 6.97 (d,  $J = 8.4$  Hz, 2H), 6.93 (d,  $J = 8.4$  Hz, 2H), 5.39 (s, 2H), 4.57 (q,  $J = 7.0$  Hz, 2H), 3.29 (d,  $J = 7.8$  Hz, 2H), 2.61 (t,  $J = 7.5$  Hz, 2H), 2.24 (s, 3H), 1.38 (t,  $J = 7.1$  Hz, 3H).  $^{13}\text{C}$  NMR (151 MHz, DMSO- $d_6$ )  $\delta$  166.25, 157.19, 140.45, 140.37, 137.66, 135.98, 135.68, 134.37, 130.26, 130.00, 129.95, 129.00, 128.31, 128.28, 127.89, 127.13, 126.00, 123.09, 120.88, 120.04, 119.92, 118.46, 65.71, 44.93, 40.20, 33.73, 20.02, 13.82. HRMS (ESI)  $m/z$  calcd  $\text{C}_{33}\text{H}_{31}\text{N}_7\text{O}_2$   $[\text{M}+\text{H}]^+$  558.2617, found 558.2583.

4.3.31. 1-((2'-(1H-tetrazol-5-yl)-[1,1'-biphenyl]-4-yl)methyl)-N-(2-(benzo[d][1,3]dioxol-5-yl)ethyl)-2-ethoxy-1H-benzo[d]imidazole-7-carboxamide (**42**)

White solid, yield 87%, mp = 189–191 °C.  $^1\text{H}$  NMR (400 MHz,  $\text{CDCl}_3$ )  $\delta$  7.88 (d,  $J = 7.4$  Hz, 1H), 7.55 (d,  $J = 6.4$  Hz, 1H), 7.49–7.37 (m, 2H), 7.34 (d,  $J = 7.6$  Hz, 1H), 7.09–6.96 (m, 4H), 6.82 (d,  $J = 8.0$  Hz, 2H), 6.68 (d,  $J = 7.8$  Hz, 1H), 6.58 (d,  $J = 8.0$  Hz, 2H), 6.44 (s, 1H), 6.30 (t,  $J = 5.7$  Hz, 1H), 5.85 (t,  $J = 5.0$  Hz, 2H), 5.27 (d,  $J = 21.7$  Hz, 2H), 4.59 (q,  $J = 7.0$  Hz, 2H), 3.43 (dd,  $J = 12.8, 6.7$  Hz, 2H), 2.68 (t,  $J = 6.8$  Hz, 2H), 1.42 (t,  $J = 7.1$  Hz, 3H).  $^{13}\text{C}$  NMR (151 MHz, DMSO- $d_6$ )  $\delta$  166.32, 159.96, 157.22, 146.79, 146.54, 145.40, 144.86, 140.44, 140.20, 139.39, 134.47, 132.71, 131.35, 130.44, 129.78, 129.39, 128.93, 128.54, 126.82, 126.17, 125.29, 121.13, 121.10, 120.94, 119.98, 119.85, 118.37, 108.47, 108.43, 107.72, 107.45, 100.24, 100.01, 65.71, 40.30, 33.81, 32.23, 13.85. HRMS (ESI)  $m/z$  calcd  $\text{C}_{33}\text{H}_{29}\text{N}_7\text{O}_4$   $[\text{M}+\text{H}]^+$  588.2359, found 588.2358.

4.3.32. 1-((2'-(1H-tetrazol-5-yl)-[1,1'-biphenyl]-4-yl)methyl)-N-(2-chlorophenethyl)-2-ethoxy-1H-benzo[d]imidazole-7-carboxamide (**43**)

Brown solid, yield 75%, mp = 187–190 °C.  $^1\text{H}$  NMR (400 MHz,  $\text{CDCl}_3$ )  $\delta$  8.03–7.95 (m, 1H), 7.54 (p,  $J = 7.3$  Hz, 2H), 7.38–7.28 (m, 3H), 7.16 (dd,  $J = 6.9, 3.7$  Hz, 4H), 7.06–6.96 (m, 2H), 6.93 (d,  $J = 8.1$  Hz, 2H), 6.78 (d,  $J = 7.9$  Hz, 2H), 5.93 (s, 1H), 5.38 (s, 2H), 4.44 (q,  $J = 7.0$  Hz, 2H), 3.50–3.38 (m, 2H), 2.87 (t,  $J = 7.0$  Hz, 2H), 1.48–1.41 (t,  $J = 7.1$  Hz, 3H).  $^{13}\text{C}$  NMR (151 MHz, DMSO- $d_6$ )  $\delta$  166.31, 157.20, 140.47, 140.35, 137.76, 136.16, 135.93, 132.53, 130.49, 130.15, 129.99, 129.93, 129.01, 128.64, 128.34, 127.60, 127.11, 126.62, 125.99, 123.32, 120.77, 120.07, 119.91, 118.53, 65.72, 44.95, 38.18, 31.95, 13.86. HRMS (EI)  $m/z$  calcd  $\text{C}_{32}\text{H}_{28}\text{ClN}_7\text{O}_2$   $[\text{M}+\text{H}]^+$  578.2071, found 578.2004.

4.3.33. 1-((2'-(1H-tetrazol-5-yl)-[1,1'-biphenyl]-4-yl)methyl)-N-(4-chlorophenethyl)-2-ethoxy-1H-benzo[d]imidazole-7-carboxamide (**44**)

White solid, yield 68%, mp = 197–199 °C.  $^1\text{H}$  NMR (400 MHz,  $\text{CDCl}_3$ )  $\delta$  7.95 (d,  $J = 7.0$  Hz, 1H), 7.51 (dtd,  $J = 13.7, 7.5, 6.1$  Hz, 2H), 7.40–7.36 (m, 1H), 7.34–7.30 (m, 1H), 7.24 (d,  $J = 8.3$  Hz, 2H), 7.20–7.12 (m, 1H), 7.09 (d,  $J = 8.3$  Hz, 2H), 7.06–6.98 (m, 2H), 6.95 (d,  $J = 8.2$  Hz, 2H), 6.81 (d,  $J = 8.0$  Hz, 2H), 6.08 (s, 1H), 5.37 (s, 2H),

4.54 (q,  $J = 7.1$  Hz, 2H), 3.43 (dd,  $J = 13.2, 6.8$  Hz, 2H), 2.76 (t,  $J = 7.0$  Hz, 2H), 1.46 (t,  $J = 7.1$  Hz, 3H).  $^{13}\text{C}$  NMR (151 MHz, DMSO- $d_6$ )  $\delta$  166.31, 157.21, 140.45, 139.87, 138.92, 137.93, 135.21, 130.08, 130.04, 129.97, 129.93, 129.89, 129.64, 128.96, 128.54, 128.43, 127.94, 127.62, 127.58, 126.64, 125.58, 120.92, 119.97, 119.89, 118.44, 65.71, 44.91, 39.81, 33.40, 13.83. HRMS (ESI)  $m/z$  calcd  $\text{C}_{32}\text{H}_{28}\text{ClN}_7\text{O}_2$   $[\text{M}+\text{H}]^+$  578.2071, found 578.2020.

4.3.34. 1-((2'-(1H-tetrazol-5-yl)-[1,1'-biphenyl]-4-yl)methyl)-N-(2,4-difluorophenethyl)-2-ethoxy-1H-benzo[d]imidazole-7-carboxamide (**45**)

Brown solid, yield 87%, mp = 199–201 °C.  $^1\text{H}$  NMR (400 MHz,  $\text{CDCl}_3$ )  $\delta$  8.00 (d,  $J = 7.0$  Hz, 1H), 7.57–7.49 (m, 2H), 7.33 (d,  $J = 6.0$  Hz, 2H), 7.15 (dd,  $J = 15.0, 8.3$  Hz, 1H), 7.04 (dd,  $J = 8.6, 5.2$  Hz, 2H), 6.98 (d,  $J = 8.1$  Hz, 2H), 6.87–6.72 (m, 5H), 6.02 (s, 1H), 5.39 (s, 2H), 4.53 (q,  $J = 7.0$  Hz, 2H), 3.43 (dd,  $J = 13.0, 6.6$  Hz, 2H), 2.79 (t,  $J = 6.8$  Hz, 2H), 1.47 (t,  $J = 6.7$  Hz, 3H).  $^{13}\text{C}$  NMR (151 MHz, DMSO- $d_6$ )  $\delta$  166.34, 161.24, 161.16, 160.88, 160.80, 159.63, 159.54, 159.25, 159.17, 157.22, 155.33, 140.47, 140.26, 138.04, 135.77, 131.59, 131.54, 131.48, 129.97, 129.86, 129.80, 129.00, 128.35, 127.01, 125.90, 124.19, 121.78, 121.76, 121.68, 120.79, 119.98, 119.93, 118.52, 110.70, 110.67, 110.56, 110.53, 103.18, 103.00, 102.83, 65.73, 44.95, 27.15, 13.82. HRMS (ESI)  $m/z$  calcd  $\text{C}_{32}\text{H}_{27}\text{F}_2\text{N}_7\text{O}_2$   $[\text{M}+\text{H}]^+$  580.2273, found 580.2272.

4.3.35. N-(2-(1H-indol-3-yl)ethyl)-1-((2'-(1H-tetrazol-5-yl)-[1,1'-biphenyl]-4-yl)methyl)-2-ethoxy-1H-benzo[d]imidazole-7-carboxamide (**46**)

Brown solid, yield 78%, mp = 189–192 °C.  $^1\text{H}$  NMR (400 MHz, DMSO- $d_6$ )  $\delta$  10.82 (s, 1H), 8.45 (t,  $J = 5.5$  Hz, 1H), 7.62 (d,  $J = 7.3$  Hz, 1H), 7.58–7.47 (m, 4H), 7.37 (d,  $J = 7.0$  Hz, 2H), 7.33 (d,  $J = 8.0$  Hz, 1H), 7.14 (s, 1H), 7.13–7.08 (m, 2H), 7.09–7.03 (m, 1H), 6.94 (q,  $J = 8.6$  Hz, 5H), 5.41 (s, 2H), 4.57 (q,  $J = 7.0$  Hz, 2H), 3.39 (d,  $J = 11.0$  Hz, 2H), 2.83–2.73 (m, 2H), 1.38 (t,  $J = 7.1$  Hz, 3H).  $^{13}\text{C}$  NMR (151 MHz, DMSO- $d_6$ )  $\delta$  166.29, 157.19, 140.44, 140.27, 137.88, 135.85, 135.63, 133.89, 129.96, 129.91, 128.99, 128.32, 127.03, 126.92, 126.60, 125.95, 122.01, 120.30, 120.08, 119.91, 118.42, 117.63, 117.60, 111.13, 110.77, 65.70, 44.92, 28.40, 24.17, 13.83. HRMS (ESI)  $m/z$  calcd  $\text{C}_{34}\text{H}_{30}\text{N}_8\text{O}_2$   $[\text{M}+\text{H}]^+$  583.2570, found 583.2571.

#### 4.4. Cell culture and reagents

A549, H1299 human lung cancer cells, 16H6E and BEAS-2B human normal lung epithelial cells were obtained from the American Type Culture Collection (Manassas, Virginia) and passaged six times before use. Cultured in Dulbecco's modified Eagle's medium (Hyclone, Logan, UT), which contains 10% fetal bovine serum (Biochrom AG, Berlin, Germany) and 100 units  $\text{ml}^{-1}$  penicillin/streptomycin solution, and store in a humidified atmosphere at 37 °C, and 5%  $\text{CO}_2$  (standard culture conditions). MLN4924, CDC and derivatives 2–48 were dissolved in dimethyl sulfoxide (DMSO) and maintained at –20 °C for *in vitro* studies. *In vivo* studies MLN4924, CDC and derivative 2–47 were dissolved in 5% 2-hydroxypropyl- $\beta$ -cyclodextrin and 5% castor oil (Macklin reagent, Shanghai, China) for *in vivo* study. MLN4924, CDC and derivatives 2–47 are all freshly prepared when used.

#### 4.5. Enzyme-based neddylation activity assay

The protein Nedd8, NAE, Ubc12, Rbx1/Cullin1<sup>CTD</sup> were prepared and gifted by Prof. Jin Huang, Shanghai Jiao Tong University School of Medicine, China. The procedure of enzyme-based assay detailed as below: 1  $\mu\text{L}$  UBA3-NAE (final concentration, 0.025  $\mu\text{M}$ ), 1  $\mu\text{L}$  Nedd8 (final concentration, 10  $\mu\text{M}$ ), 1  $\mu\text{L}$  Ubc12 (final concentration, 1  $\mu\text{M}$ ), 1  $\mu\text{L}$  RBX1/cullin1<sup>CDT</sup> (final concentration, 1  $\mu\text{M}$ ), 1  $\mu\text{L}$  Tris-

HCl (1 M, pH = 7.4; final concentration, 50 mM), 1  $\mu$ L MgCl<sub>2</sub> (0.1 M), 1  $\mu$ L DTT (10 mM), 0.2  $\mu$ L 0.1 mg/mL BSA, 2.8  $\mu$ L ddH<sub>2</sub>O, were added into each well of 96-well plates, followed with 2.0  $\mu$ L water solution of MLN4924 (final concentration, 1  $\mu$ M) or test drugs (final concentration, 50  $\mu$ M). 4.0  $\mu$ L (final concentration, 20  $\mu$ M) ATP was added to reaction after the mixture was incubated for 10 min at room temperature. The mixture was incubated at 37 °C for 30 min. The reaction was quenched by 10% loading buffer, and heated for 5 min at 95 °C by a real-time PCR. Protein samples were electrophoresed under non-reducing conditions on a 10–15% SDS-PAGE gel, and cullin1-Nedd8 levels were determined by immunoblotting analysis. To determine the neddylation inhibitory activities of **35**, **39**, **46** and CDC, various concentrations of groups were used by two-thirds decrease.

#### 4.6. Cell-based neddylation activity assay

A549 cells were exposed to the specified concentrations of MLN4924 (1  $\mu$ M) or CDC, **35**, **39** and **46** (75  $\mu$ M, 50  $\mu$ M, 32  $\mu$ M, 25  $\mu$ M, 18  $\mu$ M, 12.5  $\mu$ M, 9  $\mu$ M, 6.25  $\mu$ M and 4.5  $\mu$ M) or 0.1% (v/v) DMSO was performed for 6 h or 12 h, respectively. Cells were washed 3 times with ice-cold PBS, resuspended in RIPA lysis buffer, and incubated on ice for 30 min. Centrifuge at 15,000 rpm for 10 min at 4 °C to remove cell debris. The protein concentration of the supernatant was determined using a Thermo Fisher protein assay dye reagent (Thermo Fisher). The same amount of protein was electrophoresed on SDS-PAGE under non-reducing (cullin1-Nedd8, cullin2-Nedd8, cullin3-Nedd8, cullin4a-Nedd8 and cullin5-Nedd8) or reduced (Wee1 or p27) conditions and execute Western blot analysis.

#### 4.7. Cell apoptosis assays and cell proliferation

The FITC Annexin V Apoptosis detection kit was used to evaluate the apoptosis of A549 cells. A549 cells were seeded at  $2.5 \times 10^5$  cells per well in 6-well plates and allowed to attach overnight. Cells were treated with successively increasing concentrations of **35** (10  $\mu$ M, 20  $\mu$ M, 40  $\mu$ M) for 48 h. Cells were dissociated using trypsin, washed 3 times with ice-cold PBS buffer, and resuspended in 100  $\mu$ L of 1x binding buffer. Add 5  $\mu$ L FITC Annexin V staining solution and 5  $\mu$ L PI staining solution. After 15 min of incubation at room temperature in the dark, another 400  $\mu$ L of 1x binding buffer was added. Stained cells were immediately analyzed by fluorescence activated cell sorting (FACS).

To assess the proliferation of cultured cells, cells (A549, H1299, 16H6E, and BEAS-6B) were seeded into 96-well plates with 2500 cells per well and cultured overnight in triplicate, treated with CDC, **39**, **41**, and **47** for 48 h, and then perform Cell Counting Kit 8 (CCK-8) analysis.

#### 4.8. Molecular modeling

The X-ray structure of NAE protein was downloaded from the protein database (PDB ID: 3GZN). Removal of crystal water, ligands and other conformations through the protein preparation protocol in Autodock 4.0. The docking process between small molecule and NAE is performed through the DOCK program in Autodock 4.0, and finally the structure image is obtained using PyMOL software.

#### 4.9. Tumor xenograft growth inhibition

The animal handling and experiment protocols were approved by the Institutional Animal Care and Use Committee of Longhua Hospital Shanghai University of Traditional Chinese Medicine (2019-N038). According to the tumor transplantation protocol,

female nude mice were subcutaneously injected with 100  $\mu$ L of PBS buffer containing  $2 \times 10^6$  A<sup>549</sup> cells. After tumor induction (approximately 7–9 days), nude mice were randomly divided into 5 groups: solvent group (10% 2-hydroxypropyl- $\beta$ -cyclodextrin/water solution) and positive group (CDC-30 mg/kg). The other three groups were administered compound **39** in different ways and doses: **35** (30 mg/kg) was administered intraperitoneally, and **35** (30 mg/kg, 60 mg/kg) was administered by oral gavage. All groups were treated daily once that give it five days and off two days. Mice weight and tumor volume were measured every two days. On day 32 after vaccination, all mice were sacrificed. The tumor volume and mass of each group were measured.

#### Statistical analysis

All data were reported only if at least three independent experiments showed consistent results. The data were analyzed by one-way ANOVA followed by Dunnett's test for multiple comparisons or by Student's *t*-test for single comparison. Statistical significance was established at *p* value < 0.05.

#### Supporting information

HPLC reports for the purity check of compounds 2–46, the cullin1-Nedd8 inhibitory activities of analogs 2–46 by the enzyme-based assay, survival curve of the cullin1-Nedd8 adduction after incubating with **35**, **39**, **46** and CDC, <sup>1</sup>H NMR, MASS spectra and HPLC Traces of compounds **14**, **22**, **23**, **25**, **26** and **28–33** and the intermediates.

#### Declaration of competing interest

The author declare that they have no known competing financial interests or personal relationships that could have appeared to influence the work reported in this paper.

#### Acknowledgments

This work was supported by the Chinese Minister of Science and Technology grant (2016YFA0501800), the National Natural Science Foundation of China (Grants 81872747, 21702061, 81625018, 81820108022), the Innovative Research Team of High-level Local Universities in Shanghai, the National Special Fund for State Key Laboratory of Bioreactor Engineering (2060204), and the National Key R&D Program of China (2017YFB0202600). Innovation Program of Shanghai Municipal Education Commission (2019-01-07-00-10-E00056), Program of Shanghai Academic/Technology Research Leader (18XD1403800).

#### Appendix A. Supplementary data

Supplementary data to this article can be found online at <https://doi.org/10.1016/j.ejmech.2020.112964>.

#### Abbreviations

CRLs	cullin-RING ligases
Nedd8	neuronal precursor cell-expressed developmentally down-regulated protein 8
NAE	Nedd8-activating enzyme E1
ATP	adenosine triphosphate
A2T1R	Angiotensin II type 1 receptor
I·P.	intraperitoneal injection
DMF	<i>N,N</i> -Dimethylformamide
HOBT	1-Hydroxybenzotriazole

EDCI 1-Ethyl-3-(3-dimethylaminopropyl)carbodiimide hydrochloride  
 DIPEA Ethyldiisopropylamine  
 SARs structure-activity relationships

## References

- [1] World Health Organization, Global health observatory, Geneva, <https://who.int/gho/database/en/>, 2018. (Accessed 21 June 2018).
- [2] F. Bray, J. Ferlay, I. Soerjomataram, R.L. Siegel, L.A. Torre, A. Jemal, Global cancer statistics 2018: GLOBOCAN estimates of incidence and mortality worldwide for 36 cancers in 185 countries, *CA A Cancer J. Clin.* 68 (2018) 394–424, <https://doi.org/10.3322/caac.21492>.
- [3] J. Ferlay, M. Colombet, I. Soerjomataram, C. Mathers, D.M. Parkin, M. Piñeros, A. Znaor, F. Bray, Estimating the global cancer incidence and mortality in 2018: GLOBOCAN sources and methods, *Int. J. Canc.* 144 (2019) 1941–1953, <https://doi.org/10.1002/ijc.31937>.
- [4] A. Hershko, The ubiquitin system for protein degradation and some of its roles in the control of the cell division cycle, *Cell Death Differ.* 12 (2005) 1191–1197, <https://doi.org/10.1038/sj.cdd.4401702>.
- [5] D.M. Duda, D.C. Scott, M.F. Calabrese, E.S. Zimmerman, N. Zheng, B.A. Schulman, Structural regulation of cullin-RING ubiquitin ligase complexes, *Curr. Opin. Struct. Biol.* 21 (2011) 257–264, <https://doi.org/10.1016/j.sbi.2011.01.003>.
- [6] E.S. Zimmerman, B.A. Schulman, N. Zheng, Structural assembly of cullin-RING ubiquitin ligase complexes, *Curr. Opin. Struct. Biol.* 20 (2010) 714–721, <https://doi.org/10.1016/j.sbi.2010.08.010>.
- [7] M.D. Petroski, R.J. Deshaies, Function and regulation of cullin-RING ubiquitin ligases, *Nat. Rev. Mol. Cell Biol.* 6 (2005) 9–20, <https://doi.org/10.1038/nrm1547>.
- [8] K.I. Nakayama, K. Nakayama, Ubiquitin ligases: cell-cycle control and cancer, *Nat. Rev. Canc.* 6 (2006) 369–381, <https://doi.org/10.1038/nrc1881>.
- [9] L. Gong, E.T. Yeh, Identification of the activating and conjugating enzymes of the NEDD8 conjugation pathway, *J. Biol. Chem.* 274 (1999) 12036–12042, <https://doi.org/10.1074/jbc.274.17.12036>.
- [10] R.N. Bohnsack, A.L. Haas, Conservation in the mechanism of Nedd8 activation by the human AppBp1-uba3 heterodimer, *J. Biol. Chem.* 278 (2003) 26823–26830, <https://doi.org/10.1074/jbc.M303177200>.
- [11] D. Liakopoulos, G. Doenges, K. Matuschewski, S. Jentsch, A novel protein modification pathway related to the ubiquitin system, *EMBO J.* 17 (1998) 2208–2214, <https://doi.org/10.1093/emboj/17.8.2208>.
- [12] D.T. Huang, O. Ayrault, H.W. Hunt, A.M. Taherbhoy, D.M. Duda, D.C. Scott, L.A. Borg, G. Neale, P.J. Murray, M.F. Roussel, B.A. Schulman, E2-RING expansion of the NEDD8 cascade confers specificity to cullin modification, *Mol. Cell.* 33 (2009) 483–495, <https://doi.org/10.1016/j.molcel.2009.01.011>.
- [13] L. Li, J. Kang, W. Zhang, L. Cai, S. Wang, Y. Liang, Y. Jiang, X. Liu, Y. Zhang, H. Ruan, G. Chen, M. Wang, L. Jia, Validation of NEDD8-conjugating enzyme UBC12 as a new therapeutic target in lung cancer, *EBioMedicine* 45 (2019) 81–91, <https://doi.org/10.1016/j.ebiom.2019.06.005>.
- [14] V.N. Podust, J.E. Brownell, T.B. Gladysheva, R.S. Luo, C. Wang, M.B. Coggins, J.W. Pierce, E.S. Lightcap, V. Chau, A Nedd8 conjugation pathway is essential for proteolytic targeting of p27Kip1 by ubiquitination, *Proc. Natl. Acad. Sci. U. S. A.* 97 (2000) 4579–4584, <https://doi.org/10.1073/pnas.090465597>.
- [15] A. Kobayashi, M.-I. Kang, H. Okawa, M. Ohtsuji, Y. Zenke, T. Chiba, K. Igarashi, M. Yamamoto, Oxidative stress sensor Keap1 functions as an adaptor for cul3-based E3 ligase to regulate proteasomal degradation of Nrf2, *Mol. Cell Biol.* 24 (2004) 7130–7139, <https://doi.org/10.1128/mcb.24.16.7130-7139.2004>.
- [16] L. Li, M. Wang, G. Yu, P. Chen, H. Li, D. Wei, J. Zhu, L. Xie, H. Jia, J. Shi, C. Li, W. Yao, Y. Wang, Q. Gao, L.S. Jeong, H.W. Lee, J. Yu, F. Hu, J. Mei, P. Wang, Y. Chu, H. Qi, M. Yang, Z. Dong, Y. Sun, R.M. Hoffman, L. Jia, Overactivated neddylation pathway as a therapeutic target in lung cancer, *JNCI: J. Natl. Cancer Inst.* 106 (2014), <https://doi.org/10.1093/jnci/dju083>.
- [17] P. Chen, T. Hu, Y. Liang, P. Li, X. Chen, J. Zhang, Y. Ma, Q. Hao, J. Wang, P. Zhang, Y. Zhang, H. Zhao, S. Yang, J. Yu, L.S. Jeong, H. Qi, M. Yang, R.M. Hoffman, Z. Dong, L. Jia, Neddylation inhibition activates the extrinsic apoptosis pathway through ATF4-CHOP-DR5 Axis in human esophageal cancer cells, *Clin. Canc. Res.* 22 (2016) 4145–4157, <https://doi.org/10.1158/1078-0432.ccr-15-2254>.
- [18] H. Li, M. Tan, L. Jia, D. Wei, Y. Zhao, G. Chen, J. Xu, L. Zhao, D. Thomas, D.G. Beer, Y. Sun, Inactivation of SAG/RBX2 E3 ubiquitin ligase suppresses KrasG12D-driven lung tumorigenesis, *J. Clin. Invest.* 124 (2014) 835–846, <https://doi.org/10.1172/jci70297>.
- [19] W. Hua, C. Li, Z. Yang, L. Li, Y. Jiang, G. Yu, W. Zhu, Z. Liu, S. Duan, Y. Chu, M. Yang, Y. Zhang, Y. Mao, L. Jia, Suppression of glioblastoma by targeting the overactivated protein neddylation pathway, *Neuro Oncol.* 17 (2015) 1333–1343, <https://doi.org/10.1093/neuonc/nov066>.
- [20] Z. Luo, G. Yu, H.W. Lee, L. Li, L. Wang, D. Yang, Y. Pan, C. Ding, J. Qian, L. Wu, Y. Chu, J. Yi, X. Wang, Y. Sun, L.S. Jeong, J. Liu, L. Jia, The nedd8-activating enzyme inhibitor MLN4924 induces autophagy and apoptosis to suppress liver cancer cell growth, *Canc. Res.* 72 (2012) 3360–3371, <https://doi.org/10.1158/0008-5472.can-12-0388>.
- [21] J. Zou, W. Ma, J. Li, R. Littlejohn, H. Zhou, I.-m. Kim, D.J.R. Fulton, W. Chen, N.L. Weintraub, J. Zhou, H. Su, Neddylation mediates ventricular chamber maturation through repression of Hippo signaling, *Proc. Natl. Acad. Sci. U.S.A.* 115 (2018) E4101–E4110, <https://doi.org/10.1073/pnas.1719309115>.
- [22] W. Zhou, J. Xu, H. Li, M. Xu, Z.J. Chen, W. Wei, Z. Pan, Y. Sun, Neddylation E2 UBE2F promotes the survival of lung cancer cells by activating CRL5 to degrade NOXA via the K11 linkage, *Clin. Canc. Res.* 23 (2017) 1104–1116, <https://doi.org/10.1158/1078-0432.CCR-16-1585>.
- [23] Y. Zhao, M.A. Morgan, Y. Sun, Targeting Neddylation pathways to inactivate cullin-RING ligases for anticancer therapy, *Antioxidants Redox Signal.* 21 (2014) 2383–2400, <https://doi.org/10.1089/ars.2013.5795>.
- [24] T.A. Soucy, P.G. Smith, M.A. Milhollen, A.J. Berger, J.M. Gavin, S. Adhikari, J.E. Brownell, K.E. Burke, D.P. Cardin, S. Critchley, C.A. Cullis, A. Doucette, J.J. Garsey, J.L. Gaulin, R.E. Gershman, A.R. Lublinsky, A. McDonald, H. Mizutani, U. Narayanan, E.J. Olhava, S. Peluso, M. Rezaei, M.D. Sintchak, T. Talreja, M.P. Thomas, T. Traore, S. Vyskocil, G.S. Weatherhead, J. Yu, J. Zhang, L.R. Dick, C.F. Claiborne, M. Rolfe, J.B. Bolen, S.P. Langston, An inhibitor of NEDD8-activating enzyme as a new approach to treat cancer, *Nature* 458 (2009) 732–736, <https://doi.org/10.1038/nature07884>.
- [25] J.E. Brownell, M.D. Sintchak, J.M. Gavin, H. Liao, F.J. Bruzzese, N.J. Bump, T.A. Soucy, M.A. Milhollen, X. Yang, A.L. Burkhardt, J. Ma, H.-K. Loke, T. Lingaraj, D. Wu, K.B. Hamman, J.J. Spelman, C.A. Cullis, S.P. Langston, S. Vyskocil, T.B. Sells, W.D. Mallerder, I. Visiers, P. Li, C.F. Claiborne, M. Rolfe, J.B. Bolen, L.R. Dick, Substrate-assisted inhibition of ubiquitin-like protein-activating enzymes: the NEDD8 E1 inhibitor MLN4924 forms a NEDD8-AMP mimetic in situ, *Mol. Cell.* 37 (2010) 102–111, <https://doi.org/10.1016/j.molcel.2009.12.024>.
- [26] Julia I. Toth, L. Yang, R. Dahl, Matthew D. Petroski, A gatekeeper residue for NEDD8-activating enzyme inhibition by MLN4924, *Cell Rep.* 1 (2012) 309–316, <https://doi.org/10.1016/j.celrep.2012.02.006>.
- [27] P. Lu, X. Liu, X. Yuan, M. He, Y. Wang, Q. Zhang, P.-k. Ouyang, Discovery of a novel NEDD8 activating enzyme inhibitor with piperidin-4-amine scaffold by structure-based virtual screening, *ACS Chem. Biol.* 11 (2016) 1901–1907, <https://doi.org/10.1021/acschembio.6b00159>.
- [28] S. Zhang, J. Tan, Z. Lai, Y. Li, J. Pang, J. Xiao, Z. Huang, Y. Zhang, H. Ji, Y. Lai, Effective virtual screening strategy toward covalent ligands: identification of novel NEDD8-activating enzyme inhibitors, *J. Chem. Inf. Model.* 54 (2014) 1785–1797, <https://doi.org/10.1021/ci5002058>.
- [29] C.-H. Leung, D.S.-H. Chan, H. Yang, R. Abagyan, S.M.-Y. Lee, G.-Y. Zhu, W.-F. Fong, D.-L. Ma, A natural product-like inhibitor of NEDD8-activating enzyme, *Chem. Commun.* 47 (2011) 2511, <https://doi.org/10.1039/c0cc04927a>.
- [30] H.-J. Zhong, Y. Pui-Yan Ma, Z. Cheng, D. Shiu-Hin Chan, H.-Z. He, K.-H. Leung, D.-L. Ma, C.-H. Leung, Discovery of a natural product inhibitor targeting protein neddylation by structure-based virtual screening, *Biochimie* 94 (2012) 2457–2460, <https://doi.org/10.1016/j.biochi.2012.06.004>.
- [31] R. Seifert, H.-J. Zhong, H. Yang, D.S.-H. Chan, C.-H. Leung, H.-M. Wang, D.-L. Ma, A metal-based inhibitor of NEDD8-activating enzyme, *PLoS One* 7 (2012), e49574, <https://doi.org/10.1371/journal.pone.0049574>.
- [32] K.-J. Wu, H.-J. Zhong, G. Li, C. Liu, H.-M.D. Wang, D.-L. Ma, C.-H. Leung, Structure-based identification of a NEDD8-activating enzyme inhibitor via drug repurposing, *Eur. J. Med. Chem.* 143 (2018) 1021–1027, <https://doi.org/10.1016/j.ejmech.2017.11.101>.
- [33] H.-J. Zhong, W. Wang, T.-S. Kang, H. Yan, Y. Yang, L. Xu, Y. Wang, D.-L. Ma, C.-H. Leung, A rhodium(III) complex as an inhibitor of neural precursor cell expressed, developmentally down-regulated 8-activating enzyme with in vivo activity against inflammatory bowel disease, *J. Med. Chem.* 60 (2016) 497–503, <https://doi.org/10.1021/acs.jmedchem.6b00250>.
- [34] D.C. Scott, J.T. Hammill, J. Min, D.Y. Rhee, M. Connelly, V.O. Sviderskiy, D. Bhasin, Y. Chen, S.S. Ong, S.C. Chai, A.N. Goktug, G. Huang, J.K. Mondala, J. Low, H.S. Kim, J.A. Paulo, J.R. Cannon, A.A. Shelat, T. Chen, I.R. Kellsall, A.F. Alpi, V. Pagala, X. Wang, J. Peng, B. Singh, J.W. Harper, B.A. Schulman, R.K. Guy, Blocking an N-terminal acetylation-dependent protein interaction inhibits an E3 ligase, *Nat. Chem. Biol.* 13 (2017) 850–857, <https://doi.org/10.1038/nchembio.2386>.
- [35] J.T. Hammill, D. Bhasin, D.C. Scott, J. Min, Y. Chen, Y. Lu, L. Yang, H.S. Kim, M.C. Connelly, C. Hammill, G. Holbrook, C. Jeffries, B. Singh, B.A. Schulman, R.K. Guy, Discovery of an orally bioavailable inhibitor of defective in cullin neddylation 1 (DCN1)-Mediated cullin neddylation, *J. Med. Chem.* 61 (2018) 2694–2706, <https://doi.org/10.1021/acs.jmedchem.7b01282>.
- [36] H. Zhou, J. Lu, L. Liu, D. Bernard, C.-Y. Yang, E. Fernandez-Salas, K. Chinnaswamy, S. Layton, J. Stuckey, Q. Yu, W. Zhou, Z. Pan, Y. Sun, S. Wang, A potent small-molecule inhibitor of the DCN1-UBC12 interaction that selectively blocks cullin 3 neddylation, *Nat. Commun.* 8 (2017), <https://doi.org/10.1038/s41467-017-01243-7>.
- [37] H. Zhou, W. Zhou, B. Zhou, L. Liu, T.R. Churn, K. Chinnaswamy, J. Lu, D. Bernard, C.Y. Yang, S. Li, M. Wang, J. Stuckey, Y. Sun, S. Wang, High-affinity peptidomimetic inhibitors of the DCN1-UBC12 protein-protein interaction, *J. Med. Chem.* 61 (2018) 1934–1950, <https://doi.org/10.1021/acs.jmedchem.7b01455>.
- [38] S. Wang, L. Zhao, X.-J. Shi, L. Ding, L. Yang, Z.-Z. Wang, D. Shen, K. Tang, X.-J. Li, M.A.A. Mamun, H. Li, B. Yu, Y.-C. Zheng, S. Wang, H.-M. Liu, Development of highly potent, selective, and cellular active triazolo[1,5-a]pyrimidine-based inhibitors targeting the DCN1-UBC12 protein-protein interaction, *J. Med. Chem.* 62 (2019) 2772–2797, <https://doi.org/10.1021/acs.jmedchem.9b00113>.
- [39] W. Zhou, L. Ma, L. Ding, Q. Guo, Z. He, J. Yang, H. Qiao, L. Li, J. Yang, S. Yu, L. Zhao, S. Wang, H.-M. Liu, Z. Suo, W. Zhao, Potent 5-Cyano-6-phenyl-

- pyrimidin-Based derivatives targeting DCN1–UBE2M interaction, *J. Med. Chem.* 62 (2019) 5382–5403, <https://doi.org/10.1021/acs.jmedchem.9b00003>.
- [40] S. Ni, X. Chen, Q. Yu, Y. Xu, Z. Hu, J. Zhang, W. Zhang, B. Li, X. Yang, F. Mao, J. Huang, Y. Sun, J. Li, L. Jia, Discovery of candesartan cilexetic as a novel neddylation inhibitor for suppressing tumor growth, *Eur. J. Med. Chem.* 185 (2020) 111848, <https://doi.org/10.1016/j.ejmech.2019.111848>.
- [41] K. Kubo, Y. Kohara, E. Imamiya, Y. Sugiura, Y. Inada, Y. Furukawa, K. Nishikawa, T. Naka, Nonpeptide angiotensin II receptor antagonists. Synthesis and biological activity of benzimidazolecarboxylic acids, *J. Med. Chem.* 36 (1993) 2182–2195, <https://doi.org/10.1021/jm00067a016>.